Development of PTSD-like behavior in adult mice after observing an acute traumatic event

Ray X. Lee,[1,2]* Greg J. Stephens,[2,3] Bernd Kuhn[1]

Affiliations:

[1] Optical Neuroimaging Unit, Okinawa Institute of Science and Technology (OIST) Graduate University, Okinawa, Japan.

[2] Biological Physics Theory Unit, OIST Graduate University, Okinawa, Japan.

[3] Department of Physics and Astronomy, Vrije Universiteit Amsterdam, Amsterdam, The Netherlands.

* Correspondence to: rayxin.lee@oist.jp

Summary: In human post-traumatic stress disorder (PTSD), a major psychiatry challenge is how diverse stress reactions emerge after a protracted symptom-free period. Here, we study the behavioral development in mice isolated after observing an aggressive encounter inflicted upon their pair-housed partners and compared the results with those in multiple control paradigms. Compared with mice plainly isolated, mice isolated following the acute witnessing social stress gradually developed a wide range of long-term differences of their physiological conditions, spontaneous behaviors, and social interactions, including paradoxical results if interpreted in traditional ways. To address this developmental diversity, we applied fine-scale behavioral analysis to standard behavioral tests and showed that the seemingly sudden emergent behavioral differences developed gradually. Mice showed different developmental patterns in different zones of a behavior testing apparatus. However, the results of the fine-scale analysis together with state-space behavioral characterization allow a consistent interpretation of the seemingly conflicting observations among multiple tests. Interestingly, these behavioral differences were not observed if the aggressive encounter happened to a stranger mouse. Additionally, traumatized mice showed rebound responses to their partners after the long separation. In contrast, mice pair-housed with their attacked partners after the aggressive encounters still showed a difference in social interactions, while a difference in spontaneous behaviors did not occur. Accordingly, we propose that social relationship is the single common factor underlying the otherwise independent development of behavioral differences in this mouse paradigm and that the gained insights could have parallels in human PTSD development.

Introduction

Stress reactions can emerge long after the triggering event. Stress incubation describes the time interval following an aversive event during which stress reactions emerge or increase. Since the phenomenon of anxiety and fear incubation was first formulated and summarized (Diven, 1937), stress incubation has been assumed to be spontaneous in the sense that the development of behavioral changes is highly determined by internal rather than external causes (McAllister DE, 1967). The phenomenon of stress incubation has received serious clinical and research attention in human psychiatry, especially characterized in the post-traumatic stress disorder (PTSD), one of the most prevalent mental health disorders (DSM-5, 2013; DSM-III, 1980). Despite such prevalence, PTSD remains far from understood and controversial (McFarlane, 2010). The debates have even questioned the existence of PTSD (McHugh and Treisman, 2007; Walton et al., 2017), due to its diversity, inconsistency, and delayed onset of symptoms even after a protracted symptom-free period (Andrews et al., 2007; Pai et al., 2017).

To identify the psychopathological developments during stress incubation, it is beneficial to use an experimental assay with purely psychosocial manipulations on controlled subjective experiences and a homogeneous genetic background. Laboratory rodents have been used to study stress behavior and the pharmacology of stress (Calhoon and Tye, 2015; Cryan and Holmes, 2005; Kaouane et al., 2012; Tovote et al., 2015). A delay period before showing substantial stress reactions, suggesting stress incubation, was reported in the context of rodent models simulating human PTSD (Davis, 1989; Pamplona et al., 2011; Sillivan et al., 2017; Tsuda et al., 2015; Warren et al., 2013). The wide variety of aversive stimuli in these models range from acute physical stress (Balogh et al., 2002; Philbert et al., 2011) to prolonged witnessing of social defeat (Sial et al., 2016; Warren et al., 2013). Compared with mice experiencing direct social attacks, mice observing social attacks showed a more obvious phenomenon of stress incubation (Warren et al., 2013). This observation emphasizes the significance of emotional and cognitive processes, but not the direct impact of physical stress, in stress incubation (Hayes et al., 2012). Still, many major questions remain unanswered: Why do some symptoms attenuate while the others incubate? (Bryant et al., 2017, 2013) Why does a detailed difference in subjective experiences lead to dramatic variation in stress developments? (Adams and Boscarino, 2006) Why are symptoms usually treated partially within varied recovery contexts? (Harvey, 1996) Why does a treatment that rescues one's symptom even worsen the same symptom of another? (Scherer et al., 2017) Is stress incubation different from the formation, storage, and retrieval of fear memory? (Poulos et al., 2014)

To address such questions, we need a better understanding of the behavioral correlates in stress incubation. Here, we combined behavioral scenarios, analytic methods, and psychological hypotheses to study the development of stress incubation by psychobehavioral experiments in mice. We systematically, quantitatively, and longitudinally examined multiple physiological conditions (body mass, corticosterone level, brain connectome, etc.), spontaneous behaviors (light-dark box, open field, locomotion, etc.), and social interactions (female strangers, male strangers, pair-housed partners, etc.) of mice after observing acute social stress happening to their familiar partners (Figure 1A), with seven relevant control paradigms (Figure 1, B to H). Along the investigation, we introduced methods of fine-scale behavioral analysis and state-space behavioral characterization to overcome paradoxical and inconclusive results commonly observed in the traditional analyses of standard behavioral tests when the speculated emotions underlying behaviors are subtle and complex (Ramos, 2008). Lastly, we discussed a potential conceptual model of psychological framework based on our tests and observations in mouse stress incubation, which might provide insights on prevention, detection, and treatments of human PTSD development.

Results

Long-term effects emerged after acute trauma induction

To identify post-traumatic behavioral development with minimal physical impact and minimal peri-traumatic effects, we developed the following assay of an acute witnessing trauma (Figure 1A): Partnership between the male focal mouse and its male partner was established by housing them together for 3 weeks (Day-21–Day0). During this pair-housing, the mice slept together in a single nest which they built and no aggressive interaction (attacks, pursuits, and over-allogrooming) was observed. On Day0 (trauma induction), the focal mouse observed its partner being attacked by 5 different aggressor mice in succession (aggressive encounters) and stayed together with the attacked partner between each aggressive encounter (stress infiltration and resting). Importantly, the focal mouse only experienced the traumatic event by witnessing the attacks and by social communication and olfactory cues, but not through any direct physical threat, such as attack bites and pursuits from either the aggressors or its partner. After the last aggressive encounter, the focal observer mouse [Partner-Observing-Isolated (ParObsIso) mouse] was socially isolated for 4 weeks (Day0–Day28). Behavior was tested on Days -7, 1, 7, and 28.

To differentiate behavioral consequences from the trauma induction and the effects of isolation, adaptation to the tests, and aging, we first compared ParObsIso mice with a control group of mice isolated from their partners on Day0 without trauma induction [No-Scenario-Isolated (xScenIso) mice; Figure 1B]. We found that ParObsIso mice (n = 47) built nests with significantly higher walls than those constructed by xScenIso mice (n = 47) after isolation (Figure 2A). ParObsIso mice also increased their body mass in the late phase of the study (Figure 2B). Both observations indicate a long-term effect of the trauma induction.

To further explore potential physiological changes related to stress underlying the paradigm, we examined corticosterone concentrations in blood plasma. Compared with xScenIso mice, ParObsIso mice showed higher baseline plasma corticosterone level (CORT) after trauma, which reached statistical significance on Day28 (Figure 2C). In this experiment, we also compared CORT of ParObsIso mice with that of their partners, the attacked mice isolated after trauma [Directly-attacked-isolated (DirAtcIso) mice; n=5, note that 2 out of 5 mice died on Days 4 and 5, respectively, without obvious physical trauma; interestingly, such losses were not observed in the directly attacked mice which were subsequently group-housed]. The tendency of higher CORT was also observed in DirAtcIso mice which had a more obvious CORT increment during the early phase (Figure 2C), indicating that the observed differences of nest wall height and body mass may be phenotypes of stress.

To obtain indication of microstructural changes in the full brain correlated with these physiological and behavioral differences, we used diffusion tensor imaging (DTI) of brains collected on Day28 to analyze brain-wide microstructural differences (Figure 2, D to G; Supplemental Figures 1 to 4): Rather than a structural change in the hypothalamus which modulates CORT (DeMorrow et al., 2018), significant differences mainly occurred in both neocortex and hippocampus. For ParObsIso mice, compared with xScenIso mice, their DTI-based fractional anisotropy (FA; Figure 2D) was lower in anterior cerebral cortical areas including the primary somatosensory cortex, anterior cingulate cortex, and orbital cortex, but higher in posterior cerebral cortical areas including the retrosplenial cortex and the primary visual cortex. It was also higher in the hippocampus. Different measures of DTI-based water diffusivities [mean diffusivity (MD), axial diffusivity (AD), and radial diffusivity (RD); Figure 2, E to G] were generally higher in the cerebral cortex and hippocampus of ParObsIso than in xScenIso mice. Interestingly, we observed an obvious asymmetry of the brain areas: Gray matters including the cerebral cortex and hippocampus showed differences in the right brain hemisphere, while white matters including the corpus callosum, anterior commissure, and cingulum bundle showed differences in the left brain hemisphere. The asymmetry of

131 diffusivity between the right and left brain hemispheres were most significant in the amygdala
132 (right hemisphere shows higher diffusivity) and areas of the lateral cerebral cortical subnetwork
133 including dorsolateral orbital cortex and insular cortex (left hemisphere shows higher
134 diffusivity) for ParObsIso mice.

135 For long-range connections, the brains of ParObsIso mice show a significant increase
136 of structural connections between the right hippocampus (CA3 and dentate gyrus) and right
137 dorsolateral entorhinal cortex (Figure 2H) compared to the brain of xScenIso mice. While the
138 entorhinal cortex is the main interface between the hippocampus and neocortex, we further
139 tracked its long-range connections. The right dorsolateral entorhinal cortex showed
140 significantly increased connections with the right perirhinal cortex, but had significantly
141 decreased connections with the right piriform cortex (Figure 2H). Between the piriform and
142 perirhinal cortices, we found a decrease of their connections (Figure 2H). Through brain-wide
143 tracking, we revealed trauma-induced changes in the "perirhinal cortex–entorhinal cortex–
144 hippocampus" system, the "retrosplenial cortex–hippocampus" system, the "piriform cortex–
145 amyglala" system, and the "amyglala–hypothalamus" system. All of them centered at the
146 anterior cingulate cortex (ACC; Figure 2I), suggesting that the emergence of long-term
147 behavioral changes after trauma induction arise from network changes in this high-level
148 cognitive and emotional center.

149 ***Fine-scale behavioral analysis revealed gradual stress development***

150 Spontaneous behaviors in a steady environment has been taken as a representation of
151 internal states such as emotion (Archer, 1973). Behavioral tests for rodent anxiety-like
152 reactions were designed to evaluate their stress reaction against their willingness to explore
153 (e.g. light-dark box and elevated plus-maze) or their activity under conditions with a gradient
154 of uncertainty (e.g. open field). We first examined spontaneous behaviors in the light-dark box
155 test (Figure 3A; n = 8 mice for each group), where the stressor was a natural aversion to brightly
156 lit areas (Kumar et al., 2013). While the time spent in the light area did not differ significantly
157 between xScenIso and ParObsIso mice on Day1, ParObsIso mice surprisingly spent more time
158 in the light area than xScenIso mice on Days 7 and 28 (Figure 3A, left panels). This result
159 raised the following questions: (i) Did this behavioral difference start to develop immediately
160 after the traumatic event or only after a delay? (ii) What comparative emotionality does this
161 behavioral difference indicate?

162 To answer (i), we examined the positions of the mice in the light-dark box on a fine-
163 scale. Based on spatial symmetry, we analyzed T(x), the cumulative probability distribution
164 of time that the mouse spent at positions along the axis of the light-dark box (Figure 4A, top-

right scheme and the equation, and middle panels for the results). We calculated significance levels [presented as -log of p-values, -log(p)] of T(x) between ParObsIso and xScenIso populations by computing position-dependent population means and applying a two-tailed, two-sample Student's t-test (Figure 3A, bottom-middle panels). Already on Day1, ParObsIso mice showed differences in their spatial distribution, as they spent less time than xScenIso mice at the far end of the dark area. This tendency increased with time: On Day 7, ParObsIso mice spent more time in the light area close to the door compared to xScenIso, and then on Day 28 additionally on the far side of the light area. Collapsed -log(p) distributions reveal the overall gradual increase in spatial preference differences (Figure 3A, right panel). Additionally, ParObsIso mice maintained a higher locomotor speed compared to the gradually decreasing speed of xScenIso mice (Figure 3B) and showed more transfers between the boxes and shorter latencies until their first transfers from Day 1 (Figure 3C). These results indicate an onset and gradual increase of behavioral differences immediately following the trauma.

Regarding (ii), we additionally examined their behaviors in the elevated plus-maze test (Figure 4A; n = 8 mice for each group). In this test, stressors included fear of falling and exposure. After first exposure on Day-7 and separation, mice spent only a fraction of the time in the open arms of the maze, but with no significant difference between xScenIso and ParObsIso mice (Figure 4A, left panels). However, ParObsIso mice spent increasingly more time in the far end of the closed arms (Figure 4A, middle panels) and moved more slowly in the elevated plus-maze after trauma induction (Figure 4B) with longer periods of freezing and fewer entries to the central platform from the closed arms (Figure 4C). Although the gradually increasing differences between xScenIso and ParObsIso mice (Figure 4, A and B) was consistent, the opposite tendency of reactions in light-dark box and elevated plus-maze tests was seemingly paradoxical.

Seemingly conflicted results are regularly observed in traditional analyses of standard behavioral tests as the emotions underlying behaviors may be subtle and complex (Ramos, 2008; Ramos et al., 2008). To investigate possible psychological interpretation of the opposite reactions, we compared the behaviors of xScenIso and ParObsIso mice in the tests with the tested behaviors of mice injected with caffeine, which induces anxiety somatically (DSM-5, 2013), and mice after experiencing brief shocks, which induces anxiety cognitively (Bolton and Robinson, 2017), under the otherwise same experimental conditions and procedures. Reactions of cognitive anxiety are expected to be opposite of those shown in somatic anxiety (Cloninger, 1988). In addition, the behavioral characteristics of caffeine-injected mice and foot-shocked mice in standard tests remain controversial (Borsini et al., 2002; Gulick and

199 Gould, 2009; Suarez and Gallup, 1981; Wu et al., 2017), as what we also found when applying
200 traditional analyses (Figure 5, A and B). To capture behavioral characteristics that may be
201 overlooked in a subjective, low-dimensional representation, we first evaluated the local
202 likelihood of a given behavioral state (described by position, instantaneous locomotor speed,
203 instantaneous locomotor acceleration, and instantaneous velocity along the stressor-to-stressor-
204 free axis) to be recorded from caffeine-injected, foot-shocked, or non-treated mice. Behavioral
205 characteristics that are consistent within a group but varied across groups were therefore
206 quantitatively identified. By referring local likelihoods distributing across entire behavioral
207 state space (Supplemental Videos 1–6), we calculated the global likelihood of behaviors of
208 xScenIso and ParObsIso mice in a test to be caffeine-injected-like, foot-shocked-like, or non-
209 treated-like. While xScenIso mice kept showing non-treated-like behaviors in both tests
210 although their behaviors in classical analyses changed, ParObsIso mice developed caffeine-
211 injected-like behaviors in the light-dark box test and developed foot-shocked-like behaviors in
212 the elevated plus-maze test after trauma induction (Figure 5, C and D). The results suggest that
213 ParObsIso mice display more behaviors of chronic somatic anxiety when tested in the light-
214 dark box test and more behaviors of chronic cognitive anxiety when tested in the elevated plus-
215 maze test.

216 ***Different developmental components were untangled from a single behavioral test***

217 Through our fine-scale behavioral analyses, we further observed that, in the light-dark
218 box and elevated plus-maze tests, key incubation features were consistently more obvious
219 within stressor-free zones (dark area and closed arms) than within stressor zones (light area
220 and open arms). To quantitatively investigate the differences between zones, we analyzed
221 locomotor speed, as an independent behavioral index of mouse position, separately in stressor-
222 free and stressor zones (Figure 6). As expected, two different behavioral patterns developed
223 in the two zones: While speed differences consistently increased in stressor-free zones (Figure
224 6, B and D), speed differences in stressor zones only showed acute increases on Day1 (Figure
225 6, A and C). These results suggest that different psychological components may be measured
226 in the two zones.

227 Fear is a response to a known threat with a magnitude that increases with the strength
228 of the threat, whereas anxiety is a response to uncertainty with a magnitude that increases with
229 the uncertainty of a situation (Grupe and Nitschke, 2013). To better understand if these two
230 developmental patterns observed under and close to the stressor may be uncertainty-related,
231 we examined mouse locomotor speed in relatively uncertain and secure environments
232 separately, using the open field test (Figure 7, A to C; n = 8 mice for each group) and the

233 locomotor activity test (Figure 7D; n = 8 mice for each group). In the open field test, mice
234 were exposed to a dimly lit environment with a gradient of spatial uncertainty from the field
235 center (high uncertainty) to the field boundaries (low uncertainty). In the locomotor activity
236 test, mice were habituated in a dark and smaller environment with familiar cues of bedding
237 materials from their homecages indicative of less environmental stress. Compared to xScenIso
238 mice, ParObsIso mice moved faster in the center region of the open field (Figure 7A), which
239 was not observed in the periphery (Figure 7B). The difference between groups increased
240 gradually towards the center but not in the periphery (Figure 7, A and B). The avoidance of
241 spatial uncertainty by ParObsIso mice was also reflected in the shorter time they spent near the
242 center (Figure 7C, left panel) and showed a shorter latency to the first rearing during the test
243 (Figure 7C, right panel). In contrast, ParObsIso mice moved significantly slower on Day1 in
244 the locomotor activity test and recovered on Days 7 and 28 (Figure 7D), suggesting an acute
245 post-traumatic impact under low stress condition. These results suggest a possibility that the
246 differences of uncertainty-related spontaneous behaviors incubate, whereas that of uncertainty-
247 unrelated spontaneous behaviors attenuate.

248 ***Social differences weakly depend on emotional differences and vice versa***

249 Emotional responses simplify and speed up animal reactions to complex external cues
250 and are critical in corresponding social interactions (Anderson, 2016). To test potential
251 changes of social interactions in ParObsIso mice, we examined mouse social motivation in a
252 two-session social test (Figure 8A) where a non-social session was followed by a social session
253 (n = 5 mice for each group). The social stimulus was either a female or a male stranger mouse.
254 During the social session, ParObsIso mice spent less time in social approaches of nose poking
255 toward both female and male strangers, starting from Day1, and remained less social compared
256 to xScenIso mice during the post-traumatic period (Figure 8B). The time they spent in the
257 interaction zone around the social target, however, did not differ significantly from that of
258 xScenIso mice (Figure 8C; Supplemental Video 7). Both, ParObsIso and xScenIso mice, spent
259 only a short but similar time on nose poking during the non-social session through the
260 recordings on different days, with no significant difference between ParObsIso and xScenIso
261 populations (Figure 8D), indicating that the observed difference of nose poking time was
262 specific to social behavior. In addition, less social vocalization was recorded during the female
263 stranger test for ParObsIso mice (Figure 8E). These observations showed that trauma induction
264 also caused long-term differences in social interactions.

265 To address the relation between emotion and social cognition, we next examined how
266 the change of a particular social experience after the trauma induction could alter behavioral

development of both individual spontaneous behaviors and social interactions. An important condition in our behavioral paradigm was the forced social isolation after trauma, of which the potential effects should further be identified. We examined the impact of post-traumatic social condition on behavioral developments by the second control group of mice [Partner-Observing-Partner-Pair-Housed (ParObsParPH) mice; Figure 1C] as each of them was kept pair-housed with its attacked partner after trauma induction. Noteworthily, developments of the differences in spontaneous behaviors did not occur in ParObsParPH mice (Figure 9A, upper panels; Supplemental Figure 5A), but importantly, developments of behavioral differences in social interactions showed the differences of ParObsIso mice (Figure 9B, left panel). This observation implies the sufficiency of socially isolated condition for differences of individual spontaneous behaviors but not for that of social interactions, suggesting a weak inter-relationship between the development of emotional differences and that of social differences.

ParObsParPH mice experienced the same scenario of trauma induction as ParObsIso mice but had different post-traumatic social experiences, leading to a partial rescue of differences in spontaneous behaviors. To test the potential significance of the post-traumatic social factor in behavioral developments, we conducted two additional control experiments by alternating the post-traumatic environmental and physiological conditions, respectively, with the third control group of mice where each of them was provided with toys during social isolation after trauma induction [Partner-Observing-Isolated-Environment-Enriched (ParObsIsoEE) mice; Figure 1D], and the fourth control group of mice [Partner-Observing-Isolated-Fluoxetine-Treated (ParObsIsoFLX) mice; Figure 1E] as each of them was injected with fluoxetine daily after trauma. ParObsIsoEE mice showed similar nose poking times in the female stranger test as xScenIso mice (Figure 9B, middle panel); however, they showed the behavioral differences of ParObsIso mice in the light-dark box test, which even had a stronger difference starting from the early phase (Figure 9A, middle panels). For ParObsIsoFLX mice, while they showed less behavioral difference during the early post-traumatic phase in the light-dark box test (Figure 9A, bottom panels) and did not display a reduction of nose poking times in the female stranger test (Figure 9B, right panel), their behavioral difference in the light-dark box test reached significance in the late phase and the behavioral difference in elevated plus-maze test was more obvious in the closed arms after trauma induction (Figure 9A, bottom panels; Supplemental Figure 6A). The partial recusing and even partial strengthening of behavioral differences observed from these experimental alterations of post-traumatic social and non-social factors emphasize the sensitivity and complexity of context-wide behavioral development over stress incubation.

302 ***Social relationship determined context-wide behavioral development over stress incubation***

303 To address the psychobehavioral basis of stress incubation underlying the complexity
304 of context-wide behavioral developments that may be weakly inter-dependent, we conducted
305 the fifth control experiment where each of the mice was kept pair-housed with a stranger after
306 trauma induction [Partner-Observing-Stranger-Pair-Housed (ParObsStrPH) mice; Figure 1F],
307 altering the post-traumatic social relationship in the ParObsParPH paradigm. In the
308 ParObsStrPH paradigm, if the pair-housed strangers were the socially defeated intruders of the
309 trauma inductions, we observed aggressive attacks toward strangers by all focal mice (n=5 out
310 of 5) during their pair-housing after trauma. Similar aggression was observed among
311 ParObsIso mice, but not toward their defeated partners, when they were group-housed after
312 trauma induction. Because of these observations of partnership-dependent aggressive or non-
313 aggressive behaviors, we only conducted in-depth behavioral tests with the ParObsStrPH mice
314 pair-housed with non-defeated strangers and recorded their behavior. ParObsStrPH mice did
315 not display the development of behavioral differences in the light-dark box, elevated plus-maze,
316 and female stranger tests (Figure 10A, upper panels; 10B, left panel; Supplemental Figure 6B).
317 Only their position in the light-dark box test showed an acute difference (Figure 10A, upper
318 panels). These results indicate that a single factor of social relationship after trauma induction
319 may govern context-wide developments into long-term behavioral differences.

320 Following the evidence that social relationship governs the behavioral development
321 after the trauma induction, we further examined potential contribution of social experience on
322 trauma induction by conducting two additional control experiments with the alternation of
323 social factors during trauma induction. In the sixth control group of mice [Non-Aggressor-
324 Exposed-Isolated (xAggrExpIso) mice; Figure 1G], the aggressor mice for trauma induction
325 were replaced by non-aggressive strangers. xAggrExpIso mice did not show the developments
326 of behavioral differences in both spontaneous behaviors (Figure 10A, bottom panels) and social
327 interactions (Figure 10B, right panel), confirming that, instead of the increased number of mice
328 during trauma induction (visual exposure to 5 different aggressors), social aggression is
329 necessary to induce development of behavioral differences.

330 For the seventh group of mice [Stranger-Observing-Isolated (StrObsIso) mice; Figure
331 1H], each of the mice observed different stranger mice being attacked by different aggressors
332 and stayed together with each stranger between aggressive encounters before isolation.
333 StrObsIso mice did not experience any physical stress from strangers or aggressors. During
334 trauma induction, two notable behavioral differences were observed: While tail rattling during
335 aggressive encounters and hiding under bedding material with the partner during resting were

observed in 83% (n = 39 out of 47 mice) and 100% (n = 47 out of 47 mice) ParObsIso mice (Supplemental Video 8), respectively, no such behaviors were shown by StrObsIso mice (n = 0 out of 20 mice; n = 0 out of 20 mice). In ParObsIso mice, the frequency of tail rattles dropped progressively during aggressive encounters (Figure 11A), representing a transient reaction during trauma induction. These results suggest that social relationship may rapidly modulate emotional impact and social reactions during the trauma induction. Moreover, chronic behavioral differences were not observed in StrObsIso mice (Figure 11, B to F), which further excluded potential effects from salient, non-specific environmental manipulation (e.g. rotation through aggressors' home cages) and sensory shock (e.g. olfactory cues from urine and vocalization indicating fear) during trauma induction. Taken together, these results show that social relationship constitutes as a critical factor of trauma induction and its following context-wide developments of behavioral differences.

Considering social relationship as the key factor, an important question remained: Why did behavioral differences in the putatively uncertainty-related component of spontaneous behaviors gradually increase during stress incubation, but not remain constant or attenuate? To address this issue, we examined the persistence of social memory in a partner-revisiting test on Day28 (Figure 12A; n = 5 mice for each group). Social stimuli were the previous partner and a stranger mouse, both immobilized to allow enough social cues to be attractive, but no active interaction with the focal mouse. To avoid possible influences of social cues from socially defeated mice, stranger mice used to test xScenIso and StrObsIso mice were partners of ParObsIso mice. Strikingly, ParObsIso mice as well as ParObsIsoPH mice, which were separated from their partners right before their partners got immobilized for the tests, spent three times as much time allogrooming or pushing their previous partners as did xScenIso, xAggrExpIso, and StrObsIso mice (Figure 12B and Supplemental Video 9). The preference of ParObsIso mice to their previous partners, together with the contribution of social relationship to context-wide developments of behavioral differences after separation, implies that the uncertainty of partnership may be a key mechanism of the gradually increasing difference in uncertainty-related behaviors in our paradigm.

Discussion

We present an approach to interpret otherwise challenging and inconclusive behavioral data and use it to study stress incubation in laboratory mice. The results demonstrate a system-level view of experimentally disentangled components, processes, and determinants in stress development. We report the asymmetry of brain-wide microstructural changes and the

370 strengthening of an ACC-centered network in mice after acute witnessing social stress. Based
371 on the context-wide observations from our experiments, we propose that social relationship, as
372 the single common factor, may underlie the otherwise independent development of stress
373 incubation. Our study provides technical and conceptual advances which could be considered
374 in the study of human psychiatry disorders such as PTSD.

375 ***Detection and identification of animal emotion***

376 We argue that classical behavioral analyses of standard tests can be too coarse to
377 capture intricate emotional states. The traditional approach to identify animal emotion is to
378 test if animals show particular behaviors specified by the experimental test assumed when it
379 was designed (Walf and Frye, 2007). However, experimental animals normally display
380 obvious but not inter-supporting behaviors in different tests with the same logic and
381 assumptions (Ramos, 2008). Furthermore, even if the behavioral results are consistent with
382 the expectation, they can still be alternatively explained (Garcia et al., 2008). This ambiguity
383 reaches deeply into the history of widely used behavioral tests and therefore have resulted in a
384 considerable amount of inconclusive and seemingly paradoxical results, which are usually left
385 for discussion or remain unreported (Carobrez and Bertoglio, 2005; Crusio, 2013; Engin and
386 Treit, 2008; Ennaceur, 2014; Hascoët et al., 2001; Henriques-Alves and Queiroz, 2016;
387 Kulesskaya and Voikar, 2014). The limitations can be due to circular arguments embedded in
388 a reductive logic. Classically, researchers addressed the difficulties by an effort to show a
389 proof-of-concept (Vasconcelos et al., 2012). Therefore, studies frequently use multiple tests
390 to assess the same psychological phenomenon. With this approach, research on animal emotion
391 usually emphasize their ability to show human behavioral and physiological conditions (face
392 validity), to reproduce pharmacological effects in human (predictive validity), and to share the
393 same biological processes as human (construct validity) (Calhoon and Tye, 2015), although a
394 few studies have taken the possibility of human-unique, animal-unique, and human-animal-
395 sharing emotions under consideration (Anderson and Adolphs, 2014). To date, for the long
396 and widely used behavioral tests, a standardized method objectively identifies and quantifies
397 emotion from a continuous, high-dimensional state-space of behaviors is still absent.

398 In this study, we introduced fine-scale behavioral analysis and state-space behavioral
399 characterization to access animal emotion from standard behavioral tests which give
400 inconclusive results when analyzed and interpreted in the traditional way. Taking our
401 observations as an example, higher nest wall (Figure 2A), higher baseline corticosterone levels
402 (Figure 2C), more time spent in the far end of closed arms (Figure 4A), less exploration from
403 closed arms to center (Figure 4C, left panel), longer freezing time (Figure 4C, right panel), and

404 slower locomotion (Figure 4B) in the elevated plus-maze test, more time spent in the center
405 region (Figure 7C, left panel), and shorter latency to the first rearing (Figure 7C, right panel)
406 in the open field test, slower locomotion in the locomotor activity test (Figure 7D), and less
407 nose poking (Figure 8B) and vocalization (Figure 8E) in the stranger tests are classically more
408 acceptable as stress reactions. However, we also note that increased body mass (Figure 2B),
409 more time spent in light area (Figure 3A), faster locomotion (Figure 3B), more transfers (Figure
410 3B, right panel), shorter latency to the first transfer (Figure 3C, right panel) in the light-dark
411 box test, spending similar time around social targets in the stranger tests (Figure 8C), and more
412 social reactions to previously pair-housed partners (Figure 12B) are more controversial in
413 classic readouts. As an example, if only focusing on the observations of increased body mass
414 and higher nest wall (Figure 2, A and B), they can be interpreted as having better emotional
415 stability and therefore nicer nests and better appetites, or manifesting protective responses of
416 anxiety by hiding behind higher nest walls and engaging in anxiety-induced binge eating (Goto
417 et al., 2014; Otabi et al., 2017). Discussing potential interpretations or possible factors of these
418 massive observations can be endless and easily lead to skeptical arguments especially if the
419 focused psychobehavioral substrate is complex. With both richer measurements and
420 quantitative analyses, we were able to discover subtle behavioral differences and identify
421 otherwise obscured behavioral details in stress incubation. In addition, we propose to interpret
422 psychological meaning based on experimental comparison and correlation with physical
423 variables of the testing environment, rather than based on the expectation of presumed
424 observations, as traditionally done. Importantly, founded on computational ethology
425 (Anderson and Perona, 2014; Chen et al., 2013; Nath et al., 2019), providing a validly
426 consistent overview of data interpretations for context-wide observations across the
427 experiments becomes possibly more reliable and more effective.

428 ***From stress incubation in mice to human PTSD development***

429 Behavioral paradigms of laboratory rodents that simulate PTSD were established to
430 expose the mechanistic insights of long-term fear memory following acute physical stress
431 (Balogh et al., 2002; Philbert et al., 2011) or learned depression after repeated social defeat
432 (Sial et al., 2016; Warren et al., 2013). The diversity of PTSD models in mice is even
433 highlighted by a paradigm of trauma-free pharmacologically-induced memory impairments in
434 mice, which was recognized as a PTSD model and further identified the corresponding
435 pathophysiological mechanism (Kaouane et al., 2012). Although witnessing social defeat
436 models in rodents were developed, an identification of post-traumatic stress incubation was

437 still challenged by significant effects of the prolonged peri-traumatic stress development from
438 the repeated trauma induction for more than a week (Patki et al., 2014; Warren et al., 2013).

439 In this study, we found little support for the common view that an association among
440 psychological states, such as emotion and social motivation, govern the developmental process
441 (Andrews et al., 2007; Bryant et al., 2017; DSM-5, 2013; DSM-III, 1980; Ehlers and Clark,
442 2000; Hayes et al., 2012; Pamplona et al., 2011; Schnyder and Cloitre, 2015; Siegmund and
443 Wotjak, 2006; Zoladz and Diamond, 2013). We observed continuous growth of the differences
444 in uncertainty-related spontaneous behaviors while that of uncertainty-unrelated spontaneous
445 behaviors had long vanished (Figures 4 to 7). The time course of substantial social differences
446 also led the substantial differences of uncertainty-related spontaneous behaviors (Figures 4, 5,
447 and 8). In addition, pair-housing with partner mice selectively rescued the increased
448 differences of spontaneous behaviors but not social differences (Figure 11), and, in contrast,
449 environmental enhancement selectively strengthen the differences of spontaneous behaviors
450 but reduced the differences in social behavior (Figure 9A, middle panels). However, even with
451 this weak behavioral correlate of different psychological aspects in stress incubation, we found
452 that there is a single factor, social relationship, commonly mediating diverse behavioral
453 developments. Alternation of a single social cognitive factor, social relationship, eliminated
454 behavioral differences from mice without traumatic experience (Figures 10 and 11).
455 Conceptualization of social support as a "stress buffer" have been proposed to explain the
456 positive association between responsive social resources in a small social network and adverse
457 effects of stressful events (Cohen and Wills, 1985). Indeed, among all rescue controls,
458 including social, environmental, or pharmacological approaches (Figure 9, C to F), pair-
459 housing with non-defeated stranger mice showed the best rescuing effects on diverse
460 behavioral developments in our paradigm (Figure 12). In the collective model (Figure 13A),
461 behaviors slowly change and influence each other during stress incubation until a new,
462 abnormal equilibrium is reached; this new equilibrium is then defined as PTSD. However,
463 based on our observations and tests, we propose that a specific internal cause and its related
464 processes play a dominant role in stress incubation. In this unitary model (Figure 13B), a single
465 common factor underlies the otherwise independent development of post-traumatic behaviors
466 in mice.

467 From DTI scanning, we also found asymmetric microstructure differences and an
468 asymmetric enhanced, ACC-centered network in the two brain hemispheres, 28 days after the
469 witnessing of social stress. This is in agreement with previous finding that the right but not the
470 left ACC controls observational fear learning in mice (Kim et al., 2012). The brain heavily

471 integrates not only external but also internal causes (Donaldson et al., 2015; Funamizu et al.,
472 2016; Kohl et al., 2018; Larkum, 2013; Lee et al., 2014; R. X. Lee et al., 2015; Matias et al.,
473 2017; Murugan et al., 2017; Remedios et al., 2017; Roome and Kuhn, 2018; Tononi et al., 2016;
474 Zelikowsky et al., 2018). The potentially slow and global change of brain dynamics may arise
475 from an altered dynamic in social bonding circuits through their interconnected nodes (Ko,
476 2017). By correlating with freezing behavior following a single scrambled foot shock in mice,
477 early inhibition of PTH2R (parathyroid hormone 2 receptor)-mediated TIP39
478 (tuberoinfundibular peptide of 39 residues) signaling in the medial amygdalar nucleus was
479 demonstrated to enhance fear memory much later (Tsuda et al., 2015). Following this line, a
480 delay in generalized avoidance was proposed developing from an amplification of fear
481 expression (Houston et al., 1999; Pamplona et al., 2011; Sillivan et al., 2017). Interestingly,
482 the connections between the piriform and perirhinal cortices decreased (Figure 2, H and I). The
483 piriform and perirhinal cortices are the two core parahippocampal structures involve in the
484 kindling phenomenon, the daily progressive increase in response severity of both
485 electrographic and behavioral seizure activity (McIntyre, 2006; McIntyre and Kelly, 2006)
486 supposedly linked to fear conditioning in rat PTSD models (Knox et al., 2012; Rau et al., 2005).
487 In human PTSD research, the amygdala, medial prefrontal cortex, and hippocampus are the
488 brain regions traditionally focused on (Shin et al., 2006), with reports emphasizing the
489 morphology of the right hippocampus (Gilbertson et al., 2002; Pavić et al., 2007). Our findings
490 extend these observations to laboratory rodent model of witnessing stress under experimental
491 conditions.

492 The medial prefrontal cortex (mPFC), which includes ACC and prelimbic cortex (PL)
493 in mice, have been reported to exhibit both functional and physiological asymmetry between
494 hemispheres. For examples, the right mPFC was reported to control the acquisition of stress
495 during hazardous experiences while the left mPFC was found to play a dominant role in
496 translating stress into social behavior (E. Lee et al., 2015). The effects of erythropoietin on
497 inhibitory synaptic transmission in the left and right PL of mice were also found to be opposite
498 (Dik et al., 2018). Furthermore, neuromodulatory systems can play an important role
499 in lateralized circuitry processing. Oxytocin receptor expression is lateralized as there are more
500 OXTR-2 receptors on the left side of the auditory cortex in adult females (Marlin and Froemke,
501 2017). Based on this asymmetric nature, an oxytocin-mediated balancing of left and right
502 cortical synaptic inhibition was reported to enable maternal behavior in mice (Marlin et al.,
503 2015). Stress-induced mesocortical dopamine activation was found for the right mPFC but not
504 the left (Sullivan and Gratton, 1998). Additionally, serotonin selectively regulates mPFC
505 callosal projection neurons (Avesar and Gulledge, 2012; Stephens et al., 2014), suggesting

specific roles of the communication between left and right mPFC although they are functionally distinct. These lateralized changes on the right side due to stress experience is consistent with our observation of the changes of cortical microstructures and fibers on the right hemisphere in mice showing PTSD-like behavior. This is comparable to the predominantly right cortical volumetric differences in human PTSD (Bremner et al., 2005; Gilbertson et al., 2002). While most mechanistic or neuronal recording studies in mice only focused on one side of the brain or simultaneously regulated both sides of the brain, our data highlight a requirement for special attention on hemisphere-specific control of cognitive and emotional processes.

Although we focused on stress incubation in mice, our work may provide several important insights to complex human psychiatry, especially PTSD development. Complex developmental trajectories of human PTSD symptoms were demonstrated with associated physiological and environmental regulators (Bryant et al., 2013), yet the combination of psychological therapy and pharmacotherapy does not provide a more efficacious treatment than psychological therapy alone (Hetrick et al., 2010; Mataix-Cols et al., 2017). Our research provides a foundation to test pharmacotherapies on a system-level that integrates multiple mechanisms underlying highly diverse behavioral consequences. The efficacy of pharmacotherapies could therefore be improved. While much remains to be considered before clinical applications, our study establishes a solid basis to uncover psychological theories for therapeutic strategies (Schnyder and Cloitre, 2015). Compared with the classic view of PTSD development as a process of complex associations (McFarlane, 2010), we propose to consider human PTSD development as a process with unitary origin. While the core factor in a unitary model of human PTSD is not necessarily social bonding, we suggest a special focus on affective bonding as the core factor for patient diagnosed with witnessing PTSD. We also expect that behavioral signs of PTSD development could be detected in humans already shortly after the traumatic event. The fine-scale behavioral analyses we introduced here provides a simple, non-invasive analytic tool to capture informative behavioral details and is not limited to laboratory animals. It opens a new window for early detection and prediction, with the potential to prevent the development into PTSD.

Limitations of the Study

Although we have conducted an in-depth investigation covering multiple dimensions of behavioral phenotype, our tests and paradigms only focus on a small part of all the possibilities of an animal facing the great uncertainty in nature and achieving countless tasks through its live. In addition, since our data did not replicate common findings of social

540 avoidance followed by social defeat stress, a "dose response" of observational stress could
541 govern this "micro-defeat" which did not result in a "standard constellation" of PTSD-like
542 behaviors in mice. Finally, individual performance across different tests and the corresponding
543 cross-testing measurement effects on stress development, as a factor may be prone to
544 systematic errors, was ruled out from our study design and not examined.

545

546 **Materials and Methods**

547 All animal experiments were approved by the Institutional Animal Care and Use
548 Committee (IACUC) in the animal facility at the Okinawa Institute of Science and Technology
549 (OIST) Graduate University, accredited by the Association for Assessment and Accreditation
550 of Laboratory Animal Care (AAALAC). All animal procedures were conducted in accordance
551 with guidelines of the OIST IACUC in the AAALAC-accredited facility.

552 ***Study design***

553 The goal of this work is to identify diverse psychological aspects, temporal patterns,
554 and associations of behavioral development in mice after a single trauma induction. Pre-
555 specified hypotheses stated that (i) development of behavioral differences is already
556 represented in behavioral details during the early post-traumatic phase, while (ii) the behavioral
557 differences of spontaneous behaviors and social interactions are inter-dependent. Our data
558 support the first pre-specified hypothesis, but not the second. All other hypotheses were
559 suggested after initiation of the data analyses.

560 We approached the research goal by developing a novel mouse model of psychosocial
561 trauma under highly controlled conditions (psychosocial manipulations, subjective experiences,
562 and genetic background) and by applying fine-scale analysis to standard behavioral tests. To
563 induce acute witnessing trauma, a pair-housed mouse observed how its partner got bullied by
564 a larger, aggressive mouse on the day of trauma induction. After this trauma, the observer
565 mouse was isolated and developed behavioral differences compared to control mice in the
566 ensuing weeks. The control groups included (i) mice isolated without experiencing trauma
567 induction, (ii) mice isolated after observing how a stranger mouse got bullied by a larger,
568 aggressive mouse, (iii) mice isolated after exposed to a non-aggressive stranger mouse, (iv)
569 mice which were pair-housed with their defeat partners after observing how its partner got
570 bullied by a larger, aggressive mouse, (v) mice which were pair-housed with strangers after
571 observing how its partner got bullied by a larger, aggressive mouse, (vi) mice isolated with
572 their environment enriched, and (vii) mice isolated with daily injections of fluoxetine. The

behavioral tests included the light-dark box test, elevated plus-maze test, open field test, locomotor activity test, active social contact test to a female stranger, active social contact test to a male stranger, and partner-revisiting test. The non-behavioral tests included the body mass measurement, nest wall height measurement, baseline corticosterone concentration test, and *ex vivo* diffusion tensor imaging.

No statistical methods were used to predetermine sample sizes. Animal numbers were determined based on previous studies (Takahashi et al., 2015). 8-week-old male C57BL/6J mice, 16-week-old female C57BL/6J mice, and 20-week-old or older male Slc:ICR mice were used. No data were excluded. No outliers were defined. Mice were from different litters. Mice were randomly paired. A focal mouse was randomly selected from each pair of mice. Mice were randomly allocated into experimental groups. Testing order among groups was counterbalanced. Strangers and aggressors were randomly assigned. All behavioral tests were conducted in quintuplicate to octuplicate sampling replicates. All behavioral tests were conducted in single to quadrupole experimental cohorts. All other records were conducted in quadruplicate to septuplicate experimental cohorts. The investigator was blinded to behavioral outcomes but not to group allocation during data collection and/or analysis.

The endpoints were prospectively selected. Partner mice were expected to get minor injuries from aggressor mice during aggressive encounters; typically, attack bites on the dorsal side of posterior trunk (Takahashi et al., 2015). The aggressive encounter and all further experiments were terminated once (i) the partner mouse showed severe bleeding or ataxia, or (ii) the aggressor mice showed abnormal attack bites on any other body part. Partner mice fulfilling criteria (i) were euthanized. Aggressor mice fulfilling criteria (ii) were not used in any further experiments. If any aggressive sign (sideways threat, tail rattle, pursuit, and attack bite) was shown by the partner mouse, all further experiments with the partner mouse, aggressor mouse, and observer mouse were terminated.

Overview

In total, 527 male C57BL/6J mice (CLEA Japan, Inc.), 49 female C57BL/6J mice (CLEA Japan, Inc.), and 33 male Slc:ICR mice (Japan SLC, Inc.; retired from used for breeding) were used in this study. In CLEA Japan, nursing females were individually housed (CL-0103-2; 165×234×118 mm), while pups were separated on P21 according to gender and housed ≤15 mice per cage (CL-0104-2; 206×317×125 mm). Pups were re-arranged on P28 according to their weights and housed ≤13 mice per cage (CL-0104-2). Mice were shipped in boxes each with 10 – 30 mice to the OIST Animal Facility. In the OIST Animal Facility, mice were housed in 380×180×160-mm transparent holding cages (Sealsafe Plus Mouse DGM - Digital Ready

607 IVC; Tecniplast Inc., Quebec, Canada) bedded with 100% pulp (FUJ9298101; Oriental Yeast
608 Co., Ltd., Tokyo, Japan) under a 12-hr dark/light cycle (350-lux white light) at a controlled
609 temperature of 22.7 – 22.9 ºC, humidity of 51 – 53%, and differential pressure of -14 – -8 Pa
610 with food and water available ad libitum. Circadian time (CT) is defined to start at mid-light
611 period and described in a 24-hr format, i.e. light off at CT 6:00.

612 The experimenter and caretakers wore laboratory jumpsuits, lab boots, latex gloves,
613 face masks, and hair nets when handling mice and performing experiments. Handling of mice
614 during the dark cycle was done under dim red light and mice were transported in a lightproof
615 carrier within the animal facility. For mice in experimental and control groups tested on the
616 same dates, the testing order was alternated. Surfaces of experimental apparatuses were wiped
617 with 70% ethanol in water and dry paper tissues after testing each mouse to remove olfactory
618 cues. Each mouse was only used for one behavioral test (in total 4 records with intervals of 6
619 – 21 days) to avoid confounded results due to cross-testing and to minimize measurement
620 effects on its psychological development (Krishnan et al., 2007).

621 ***Pre-traumatic period (Day-21 to Day0)***

622 To establish partnerships between mice, a male C57BL/6J mouse (focal mouse; 8 weeks)
623 was pair-housed with another male C57BL/6J mouse (partner mouse; 8 weeks) for 3 weeks
624 (Day-21 to Day0, with trauma induction on Day0). The partner was initially marked by ear
625 punching. The holding cage was replaced once per week, with the last change 3 days before
626 the traumatic event (Day-3).

627 To establish the territory of an aggressor mouse in its homecage, an Slc:ICR mouse
628 (aggressor mouse; ≥20 weeks) was pair-housed with a female C57BL/6J mouse (female mouse;
629 16 weeks) for 3 weeks (Day-21 to Day0). The holding cage was replaced with a clean one
630 once a week, with the last change one week before the traumatic event (Day-7).

631 Aggression level of aggressors was screened on Days -5, -3, -1 through intruder
632 encounters (Miczek and O'Donnell, 1978) toward different screening mice to determine
633 appropriate aggressors to be used for trauma induction on Day0. Aggression screening was
634 carried out in the behavior testing room at 22.4 – 23.0 ºC, 53 – 58% humidity, -4 – -3 Pa
635 differential pressure, and 57.1 dB(C) ambient noise level during the light period (CT 4:00 –
636 6:00) with 350-lux white light. After the female and pups with the aggressor were taken out of
637 their homecage and kept in a clean holding cage in the behavior testing room, a 3-min
638 aggression screening was started after a male C57BL/6J mouse (screening mouse; 10 weeks)
639 was brought into the homecage of the aggressor, followed by covering the cage with a

transparent acrylic lid. During screening, the aggressor freely interacted with the screening mouse. The aggressor was brought back to the holding room after the screening mouse was taken away from the aggressor's homecage and the female and pups were brought back to its homecage right after screening. Aggressors were selected for trauma induction on Day0 if they showed biting attacks on all of these screening days and the latencies to the initial bites on Day-3 and Day-1 were less than 20 s.

Trauma induction (Day0)

The following experimental assay emotionally introduced an acute traumatic experience in mice through a social process. The setup was the aggressor's homecage, divided into an 80×180-mm auditorium zone and a 300×180-mm battle arena by the insertion of a stainless-steel mash with 8×8-mm lattices. The cage was covered with a transparent acrylic lid. The behavioral procedure was carried out in the behavior testing room during CT 4:00 – 6:00, with 3 – 5 experiments done in parallel.

After the female and pups with the aggressor were taken out of their homecage, a divider was inserted into the aggressor's homecage, allowing the aggressor to freely behave in the battle arena, but not to enter the auditorium zone. A 5-min aggression encounter session started after the focal mouse was brought to the auditorium zone and its partner to the battle arena. Tail rattling counts of the focal mouse during aggressive encounter were recorded by experimenter. The aggressive encounter session was followed by a 5-min stress infiltration session, in which the partner was brought to the focal mouse in the auditorium zone, while the aggressor remained in the battle arena. Right after the stress infiltration session, both focal mouse and its partner were brought back to their homecage in the behavior testing room for a 10-min resting period. The procedure was repeated 5 times with different aggressors. During each resting session, the aggressor stayed in its homecage without the divider before its next intruder encounter. Each aggressor had 3 – 5 encounters with resting periods of 10 – 30 min. After the 5th aggression encounter session, the focal mouse was placed back in its homecage where the nest had been razed, and brought back to the holding room. Partners from different pairs were brought to a new holding cage and housed in groups of 3 – 5 per cage. Right after the last intruder encounter for each aggressor, the female and pups were brought back to the homecage and returned to the holding room together with the aggressor.

Post-traumatic period (Day0 to Day28)

To investigate the behavior of focal mice after trauma induction (now called ParObsIso mice, Figure 2A), they were housed individually for 4 weeks after the procedure (Day0 to

673 Day28). No environmental enrichment was provided, except to the ParObsIsoEE mice, and
674 the holding cage was not changed during social isolation.

675 ***Control experiments***

676 To differentiate behavioral consequences of the emotionally traumatic experience from
677 consequences of social isolation, a control group of mice had their partners taken away and
678 their nests razed during body weighing on Day0 without trauma induction (xScenIso mice,
679 Figure 1B).

680 To examine the potential reversal effects of social support on the emotionally traumatic
681 experience, a control group of mice was kept pair-housed with their attacked partners after
682 trauma induction (ParObsParPH mice, Figure 1C).

683 To characterize potential reversal effects through environmental factors besides social
684 factors, a control group of mice was housed individually with environmental enrichment,
685 provided with a pair of InnoDome™ and InnoWheel™ (Bio-Serv, Inc., Flemington, NJ, USA)
686 and a Gummy Bone (Petite, Green; Bio-Serv, Inc.), after trauma induction (ParObsIsoEE mice,
687 Figure 1D).

688 To demonstrate predictive validity of potential treatment on stress by an antidepressant,
689 a control group of mice was intraperitoneally injected with fluoxetine (2 µl/g of 10 mg/ml
690 fluoxetine hydrochloride dissolved in saline, i.e. 20 mg/kg; F132-50MG; Sigma-Aldrich, Inc.,
691 Saint Louis, MO, USA) once per day at CT 1:00 – 2:00 after trauma induction (ParObsIsoFLX
692 mice, Figure 1E).

693 To further test the critical component of social relationship in the potential social
694 support reversal, a control group of mice was kept pair-housed but with a stranger mouse after
695 trauma induction (ParObsStrPH mice, Figure 1F).

696 To identify the impacts of aggression during trauma induction, a control group of mice
697 experienced exposure to strangers of the same strain, gender, and age, instead of the aggressor
698 mice for trauma induction (xAggrExpIso mice, Figure 1G).

699 To test the influence of social relationship on the emotionally traumatic experience, a
700 control group of mice witnessed the traumatic events toward stranger mice of the same strain,
701 gender, and age instead (StrObsIso mice, Figure 1H). In each iteration of the aggression
702 encounter, stress infiltration, and resting period, a different stranger mouse was presented.

703 To identify anxiety-like spontaneous behaviors putatively induced by somatic
704 uncertainty, a group of mice was initially sedated with 3%v/v isoflurane in oxygen and then

705 intraperitoneally injected with caffeine (20 μl/g of 0.75 mg/ml anhydrous caffeine dissolved in
706 saline, i.e. 15 mg/kg; 06712-55; Nacalai Tesque, Inc., Kyoto, Japan). Recording of
707 spontaneous behaviors were started 30 min after the injections.

708 To identify anxiety-like spontaneous behaviors putatively induced by cognitive
709 uncertainty, a group of mice was initially sedated with 3%v/v isoflurane in oxygen and then
710 intraperitoneally injected with 2 μl/g saline. The mice received a series of foot shocks (1 mA
711 for 1 s, 6 times in 5 min, i.e. once every 50 s for the first started at 49 s after placed in the
712 chamber; single chamber system; O'Hara & Co., Ltd., Tokyo, Japan) 25 min after the injections.
713 Recording of spontaneous behaviors were started 30 min after the injections.

714 To identify non-treated-like spontaneous behaviors, a control group of mice was
715 initially sedated with 3%v/v isoflurane in oxygen and then intraperitoneally injected with 2
716 μl/g saline. Recording of spontaneous behaviors were started 30 min after the injections.

717 ***Body mass and nest wall height***

718 In the holding room, body masses of all individuals were recorded on Days -7, 0, 1, 7,
719 28, while the heights of nest walls built by each individual were recorded on Days 1, 7, 28.
720 The height of the nest wall was measured with 5-mm resolution using a transparent acrylic
721 ruler, while the mouse was weighed with 10-mg resolution on a balance. Mice were placed
722 back in their homecages right after recording.

723 ***Light-dark box test***

724 The light-dark box test is an experimental assay to measure anxiety in rodents (Crawley
725 and Goodwin, 1980), designed to evaluate their natural aversion to brightly lit areas against
726 their temptation to explore. The light-dark box setup consisted of two connected 200×200×250-
727 mm non-transparent PVC boxes, separated by a wall with a 50×30-mm door. The boxes were
728 covered with lids with white and infrared LED light illumination for the light and dark areas,
729 respectively, and CCD cameras in the centers (4-chamber system; O'Hara & Co., Ltd., Tokyo,
730 Japan). The floors of the boxes were white, while the walls of the boxes were white for the
731 light area and black for the dark area. Uniform illumination in the light area was 550 lux.
732 Behavioral tests were carried out on Days -7, 1, 7, and 28 in the behavior testing room at 22.7
733 – 23.0 ºC, 51 – 54% humidity, -11 – -9 Pa differential pressure, and 53.6 dB(C) ambient noise
734 level during dark period (CT 6:00 – 8:00).

735 After habituation for 10 min individually in the homecage in the behavior testing room
736 in darkness, the focal mouse was transferred to the dark area through a 50×50-mm side door.
737 A 5-min behavior record was started right after the side door of dark area was closed and the

door between light and dark areas was opened. Locomotion was recorded 2-dimensionally at 15 Hz from top-view with CCD video cameras. Right after recording, the mouse was returned to its homecage, and brought back to the holding room.

Elevated plus-maze test

The elevated plus-maze test is an experimental assay to measure anxiety in rodents (Pellow et al., 1985), designed to evaluate their natural fear of falling and exposure against their temptation to explore. The elevated plus-maze setup consisted of a gray PVC platform raised 500 mm above the ground (single maze system; O'Hara & Co., Ltd.). The platform was composed of a 50×50-mm square central platform, two opposing 50×250-mm open arms, and two opposing 50×250-mm closed arms with 150-mm semi-transparent walls. Each of the two open arms emanated at 90° to each of the two closed arms, and vice versa. The apparatus was installed in a soundproof box with white fluorescent lamp illumination (20 lux) and ventilators. Behavioral tests were carried out on Days -7, 1, 7, 28 in the behavior testing room at 22.8 – 23.0 ºC, 53 – 56% humidity, -13 – -11 Pa differential pressure, and 52.1 dB(C) ambient noise level during dark period (CT 8:00 – 10:00).

After habituation for 10 min individually in the homecage in the behavior testing room in darkness, the focal mouse was brought to the central platform of the elevated plus-maze, facing the open arm on the opposite side from the door of the soundproof box. A 5-min behavior recording was started right after the door of the soundproof box was closed. Locomotion was recorded 2-dimensionally at 15 Hz from top-view with a CCD video camera installed above the center of the central platform. Delineated entrances to open and closed arms were defined at 50 mm from the center of the central platform. Right after recording, the mouse was placed back in its homecage, and brought back to the holding room.

Open field test

The open field test is an experimental assay to measure anxiety in rodents (Hall and Ballachey, 1932), designed to evaluate their spontaneous activity under a gradient of spatial uncertainty (high in the field center and low along the walls and at the corners of the field). The open field setup consisted of a 400×400×300-mm non-transparent gray PVC box with no cover, installed in a soundproof box with white LED light illumination and ventilators (2-chamber system; O'Hara & Co., Ltd.). Behavioral tests were carried out on Days -7, 1, 7, 28 in the behavior testing room at 22.8 – 23.0 ºC, 53 – 56% humidity, -13 – -11 Pa differential pressure, and 56.7 dB(C) ambient noise level during dark period (CT 8:00 – 10:00).

After habituation for 10 min individually in the homecage in the behavior testing room in darkness, the focal mouse was brought to the center of the open field arena under 20-lux uniform illumination, facing the wall on the opposite side from the door of the soundproof box. A 5-min behavior recording was started right after the door of the soundproof box was closed. Locomotion was recorded 2-dimensionally at 15 Hz from top-view with a CCD video camera installed above the center of the open field arena. Vertical activity of exploratory rearing behavior was recorded by the blocking of invisible infrared beams created and detected by photocell emitters and receptors, respectively, positioned 60 mm high on the walls of the open field box. A delineated center region was defined as the central 220×220 mm area. Right after recording, the mouse was placed back in its homecage, and returned to the holding room.

Locomotor activity test

The locomotor activity test is an experimental assay to measure spontaneous activity of rodents in an environment without an experimentally designed stressor. The locomotor activity setup consisted of a 200×200×250 mm non-transparent covered PVC box with infrared LED illumination and a CCD camera in the center (the dark area of the light-dark box setup, while the door between the light and dark areas was closed and fixed). The floor of the box was embedded with bedding material from the homecage of the focal mouse, while the walls of the box were black. Behavioral test was carried out on Days -7, 1, 7, 28 in the behavior testing room at 22.7 – 23.0 ºC, 51 – 54% humidity, -11 – -9 Pa differential pressure, and 53.6 dB(C) ambient noise level during dark period (CT 6:00 – 8:00).

After habituation for 30 min individually in the behavior testing box, a 1-hr behavior recording was started. The behavior testing box was not covered completely in order to allow air circulation. Locomotion was recorded 2-dimensionally at 15 Hz from top-view with the CCD video camera. Right after recording, the mouse was returned to its homecage, and brought back to the holding room.

Active social contact test

The active social contact test [also known as "social interaction test", but to be distinguished with the one-session test using an open field with a social target freely behaving in the field (Arakawa et al., 2014) or the one-session test placing a social target-containing cylinder into the center of the testing subject's homecage for social instigation (Tsuda and Ogawa, 2012)] is a 2-session experimental assay to measure social motivation in rodents (Berton et al., 2006). The setup consists of a 400×400×300-mm non-transparent gray PVC box with no cover, installed in a soundproof box with 20-lux white LED illumination and ventilators.

A 60×100×300-mm stainless-steel chamber with wire grid sides was placed in the center of the wall on the opposite side from the door of the soundproof box. The wire grid had 8×8 mm lattices at a height of 10 – 60 mm from the bottom. An ultrasound microphone (CM16/CMPA; Avisoft Bioacoustics, Glienicke, Germany) with an acoustic recording system (UltraSoundGate; Avisoft Bioacoustics) was hung outside the chamber, 100 mm above the ground. Behavioral tests were carried out on Days -7, 1, 7, 28 in the behavior testing room at 22.8 – 23.0 ºC, 53 – 56% humidity, -13 – -11 Pa differential pressure, and 56.7 dB(C) ambient noise level during dark period (CT 8:00 – 10:00).

The social target used for active social contact tests was either a male or a female C57BL/6J mouse (18 weeks), pair-housed with a partner of the same strain, gender, and age for more than 2 weeks before the tests. The social target was adapted to the experimental protocol one day before the tests in the behavior testing room during dark period (CT 8:00 – 9:00): After habituation for 5 min individually in the homecage in the soundproof box under 20-lux uniform illumination, the social target was brought into the chamber in the open field arena under 20 lux uniform illumination. A male C57BL/6J mouse (11–16 weeks; from partners of xScenIso mice in previous experiment) was then brought to the open field arena for a 2.5-min spontaneous exploration and interaction with the social target. The social target was then brought back to its homecage in the soundproof box under 20-lux uniform light for a 5-min rest. The social interaction procedure was repeated with a different male C57BL/6J mouse right afterward. After the social target had interacted with 4 different mice, it was returned to its homecage and brought back to the holding room.

On testing days, after 10-min habituation individually in its homecage in the behavior testing room in darkness, the first session of the active social contact test started by placing the focal mouse at the center of the open field arena under 20-lux uniform light, facing the empty chamber. A 2.5-min behavior recording started right after the door of the soundproof box was closed. Locomotion was recorded 2-dimensionally at 15 Hz from top-view with a CCD video camera installed above the center of the open field arena. Ultrasonic vocalization was recorded at 250 kHz. In the second session of the active social contact test, which followed the first session, the social target was brought into the chamber. Another 2.5-min behavior recording started as soon as the door of the soundproof box was closed. Right afterward, the focal mouse was returned to its homecage and brought back to the holding room.

The focal mouse experienced active social contact tests with different social targets on different recording days (Days -7, 1, 7, 28), while different focal mice were tested with the same social target on the same recording day (5 – 10 records). The social target remained in

its homecage in a soundproof box under 20-lux uniform illumination before and between each test. A delineated interaction zone was taken as the region within 80 mm of the edges of the chamber. Social approaches of the focal mouse poking its nose toward the social target were recorded manually using the event recording software, tanaMove ver0.09 (http://www.mgrl-lab.jp/tanaMove.html).

Partner-revisiting test

The partner-revisiting test is a memory-based experimental assay to measure social bonding in rodents [sharing similar concept of "familiar *v.s.* novel social target recognition", but to be distinguished with the three-chamber paradigm test (Nadler et al., 2004)]. The partner-revisiting setup was the uncovered homecage of the focal mouse, installed in a soundproof box with white LED illumination and ventilators (O'Hara & Co., Ltd., Tokyo, Japan). The long sides of the homecage were parallel to the door of soundproof box. The partner-revisiting test was carried out on Day28 in the behavior testing room at 22.8 – 23.0 ºC, 53 – 56% humidity, -13 – -11 Pa differential pressure, and 56.7 dB(C) ambient noise level during light period (CT 4:00 – 6:00) with 350-lux light intensity.

The previously separated partner of the focal mouse, being a social target in the test, was initially sedated with 3%v/v isoflurane in oxygen, and then anesthetized by intraperitoneal (i.p.) injection of a mixture of medetomidine (domitor, 3%v/v in saline, 0.3 mg/kg), midazolam (dormicum, 8%v/v in saline, 4 mg/kg), and butorphanol (vetorphale, 10%v/v in saline,5 mg/kg). Also, a stranger mouse (15 weeks; a separated partner of a ParObsIso or Buffered mouse for testing a xScenIso, StrObsIso, or xAggrExpIso mouse, and *vice versa*) was anesthetized as an alternative social target. Both anesthetized mice were kept on a heating pad at 34ºC (B00O5X4LQ2; GEX Co., Ltd., Osaka, Japan) to maintain their body temperatures before the test.

The focal mouse was brought to a clean, uncovered holding cage in the soundproof box under 50-lux uniform illumination for 5-min habituation, while its homecage was placed in another soundproof box under 50-lux uniform light. During habituation of the focal mouse, the anesthetized social targets were injected with atipamezole hydrochloride (antisedan; 6%v/v in saline for 0.3 mg/kg, i.p.) to induce recovery from anesthesia. During the waking-up period, the social targets were still immobilized and not able to actively interact with the focal mouse during the following recording, but showed enough social cues to be attractive for the focal mouse. The immobilized social targets were then placed in the homecage of the focal mouse with their nose pointing toward the center of the short side of the wall (10 mm of nose-to-wall distance) with their bellies facing the door of the soundproof box. After habituation, the focal

871 mouse was brought to the center of its homecage, facing the long side of the homecage wall on
872 the opposite side from the door of soundproof box. A 10-min behavior record started right
873 after the door of the soundproof box was closed. Locomotion was recorded 2-dimensionally
874 at 15 Hz from top-view with a CCD video camera installed above the center of the homecage.
875 Right after recording, social targets were taken out of the focal mouse's homecage and the focal
876 mouse was brought back to the holding room.

877 Social contacts including sniffing, allogrooming, and pushing of the focal mouse
878 toward each of the social targets were recorded manually using the event recording software,
879 tanaMove ver0.09 (http://www.mgrl-lab.jp/tanaMove.html).

880 ***Baseline plasma corticosterone concentration test***

881 The baseline plasma corticosterone (CORT) concentration test is a competitive-
882 inhibition enzyme-linked immunosorbent assay (ELISA) to measure physiological stress level
883 in rodents, designed to quantitatively determinate CORT concentrations in blood plasma. The
884 sample collection was carried out on Days -7, 1, 7, 28 in the behavior testing room at 22.4 –
885 23.0 ºC, 53 – 58% humidity, -4 – -3 Pa differential pressure, and 57.1 dB(C) ambient noise
886 level during CT 4:00 – 6:00 with 350-lux white light.

887 After habituation for 30 min individually in the homecage in the behavior testing room,
888 the mouse was initially sedated with 3%v/v isoflurane in oxygen. Six drops of blood from the
889 facial vein pricked by a 18G needle were collected in a EDTA-lined tube [K2 EDTA (K2E)
890 Plus Blood Collection Tubes, BD Vacutainer; Becton, Dickinson and Company (BD), Franklin
891 Lakes, NJ, USA] and kept on ice. Right after collection, the mouse was returned to its
892 homecage, and brought back to the holding room. Whole blood samples were then centrifuged
893 (MX-300; Tomy Seiko Co., Ltd., Tokyo, Japan) at 3,000 rpm for 15 min at 4°C. Plasma
894 supernatant was decanted and kept at -80°C until the measurement on Day 29.

895 CORT concentrations in blood plasma were tested with Mouse Corticosterone (CORT)
896 ELISA Kit (MBS703441, 96-Strip-Wells; MyBioSource, Inc., San Diego, USA; stored at 4°C
897 before use) on Day 29. All reagents [assay plate (96 wells, pre-coated with goat-anti-rabbit
898 antibody), standards (0, 0.1, 0.4, 1.6, 5, and 20 ng/ml of CORT), rabbit-anti-CORT antibody,
899 HRP-conjugated CORT, concentrated wash buffer (20x phosphate-buffered saline (PBS)),
900 3,3',5,5'-tetramethylbenzidine (TMB) color developing agent (substrates A and B), and TMB
901 stop solution] and samples were brought to room temperature for 30 min before use. Collected
902 plasma samples after thawing were centrifuged again (MX-300; Tomy Seiko Co.) at 3,000 rpm
903 for 15 min at 4°C. 20 µl of standard or sample was added per well, assayed in duplicate, with

904 blank wells set without any solution. After 20 µl of HRP-conjugated CORT was added to each
905 well except to the blank wells, 20 µl of rabbit-anti-CORT antibody was added to each well and
906 mixed. After incubation for 1 hour at 37°C, each well was aspirated and washed, repeated for
907 3 times, by filling each well with 200 µl of wash buffer (diluted to 1x PBS) using a squirt bottle,
908 standing for 10 s, and completely removing liquid at each step. After the last wash and the
909 removal of any remaining wash buffer by decanting, the plate was inverted and blotted against
910 clean paper towels. After TMB color developing agent (20 µl of substrate A and 20 µl of
911 substrate B) was added to each well, mixed, and incubated for 15 min at 37°C in dark, 20µl of
912 TMB stop solution was added to each well and mixed by gently tapping the plate. The optical
913 density (O.D.) of each well was determined, within 10 min, using a microplate reader
914 (Multiskan GO; Thermo Fisher Scientific, Inc., Waltham, MA, USA) measuring absorbance at
915 450 nm, with correction wavelength set at 600–630 nm.

916 CORT concentrations were calculated from the O.D. results using custom scripts
917 written in MATLAB R2015b (MathWorks). The duplicate O.D. readings for each standard and
918 sample was averaged and subtracted the average O.D. of the blanks, $X = \langle O.D. \rangle -$
919 $\langle O.D. \rangle_{blank}$. A standard curve was determined by a four parameter logistic (4PL) regression
920 fitting the equation $\rho_{CORT}(X_{standard}) = d + \frac{a-d}{1+(\frac{X_{standard}}{c})^b}$, where ρ_{CORT} is the CORT
921 concentration, a is the minimum asymptote, b is the Hill's slope, c is the inflection point, and
922 d is the maximum asymptote. CORT concentrations of the samples were calculated from the
923 fitted 4PL equation with respected to X_{sample}.

924 ***Ex vivo diffusion tensor imaging***

925 *Ex vivo* diffusion tensor imaging (DTI) is a magnetic resonance imaging (MRI)
926 technique to determinate structural information about tissues (Basser et al., 1994), designed to
927 measure the restricted diffusion of water in tissue. The sample collection was carried out on
928 Day 28 in the necropsy room at 22.4 - 22.5 ºC, 53 - 54 % humidity, and 10 - 12 Pa differential
929 pressure during CT 4:00 - 6:00 with 750-lux white light.

930 After mice were brought individually in their homecages to the necropsy room, they
931 were initially sedated with 3%v/v isoflurane in oxygen, then deeply anaesthetized with a
932 ketamine-xylazine mixture (>30 µl/g body weight of 100 mg/ml ketamine and 20 mg/ml
933 xylazine), and perfused transcardially. The perfusates, in a two-step procedure, were (i) 20 ml
934 of ice cold 1x phosphate-buffered saline (PBS), and (ii) 20 ml of ice cold 4% paraformaldehyde,
935 0.2% sodium meta-periodate, and 1.4% lysine in PBS. Mouse skull including the brain was
936 removed and stored in the perfusate (ii) at 4 ºC for 2 weeks. Each skull with the brain was then

transferred into 2 mM gadolinium with diethylenetriaminepentaacetic acid (Gd-DTPA) and 0.5% azide in PBS for 2 weeks.

Isolated fixed brains within the skulls were positioned in an acrylic tube filled with fluorinert (Sumitomo 3M Ltd., Tokyo, Japan) to minimize the signal intensity attributable to the medium surrounding the brain during MRI scanning. All MRI was performed with an 11.7-T MRI system (BioSpec 117/11; Bruker Biospec, Ettlingen, Germany) using ParaVision 6.0.1 software (Bruker Biospec, Ettlingen, Germany) for data acquisition. The inner diameter of the integrated transmitting and receiving coil (Bruker Biospec, Ettlingen, Germany) was 35 mm for the ex vivo MRI. DTI data were acquired by using a 3-D diffusion-weighted spin-echo imaging sequence, with repetition time (TR) = 267 ms, echo time (TE) = 18.5 ms, b-value = 2,000 s/mm2, and 30 non-collinear directions. Five T2-weighted measurements were acquired together with DTI, for one every 6 diffusion measurements. The acquisition matrix was 216×216×168 over a 27.0×27.0×21.0 mm3 field of view, resulting in a native isotropic image resolution of 125 μm. Total acquisition time was 96 hr.

MRI data was processed using custom scripts written in MATLAB R2015b (MathWorks). All 30 DTI and 5 T2 3-D images were masked by thresholding at the half of mean values of diffusion weights for each voxel and omiting clusters smaller than 10 voxels. After diffusion tensor of each voxel was estimated by solving the Stejskal-Tanner equation through linear regression (Hrabe et al., 2007), the 3 eigenvalues (λ_1, λ_2, and λ_3) with respect to the 3 axes of the diffusion ellipsoid (the longest, middle, and shortest axes, respectively) were calculated by eigenvalue decomposition of the diffusion tensor. Four focused DTI-based measures (Mori, 2007) are the mean diffusivity (MD) that represents membrane density

$$MD = \langle\lambda\rangle = \frac{\lambda_1 + \lambda_2 + \lambda_3}{3},$$

axial diffusivity (AD) that represents neurite organization

$$AD = \lambda_1 ,$$

radial diffusivity (RD) that represents myelination

$$MD = \frac{\lambda_2 + \lambda_3}{2},$$

and fractional anisotropy (FA) that represents average microstructural integrity

$$FA = \sqrt{\frac{3 \times [(\lambda_1 - \langle\lambda\rangle)^2 + (\lambda_2 - \langle\lambda\rangle)^2 + (\lambda_3 - \langle\lambda\rangle)^2]}{2 \times \left({\lambda_1}^2 + {\lambda_2}^2 + {\lambda_3}^2\right)}}.$$

After the registration of these 3-D DTI-based brain maps to a template brain atlas (DSURQE Atlas; https://wiki.mouseimaging.ca/display/MICePub/Mouse+Brain+Atlases), mean values of these DTI-based quantities were identified in a total of 244 brain regions ($) for each individual. Based on the FA maps, DTI-based long-range fiber tracking from a focal seed region ($B) was calculated with 2 samplings, distance of forward fiber in one step = 50 μm, and thresholds of minimal fiber length = 750 μm, maximal fiber length = 75,000 μm, maximal fiber deviation angle = 57.3º, and minimal FA for keeping tracking = 0.4.

Video data processing

Video image data was processed using custom scripts written in MATLAB R2015b (MathWorks). Each video frame from a recorded AVI video file was read as a 2-dimensional matrix with an 8-bit gray scale. Each of these matrices was then divided by a background matrix read from a TIF image file of the background taken before bringing the test mouse to the setup. The centroid of the area with non-one values in each matrix ratio was taken as the position of the mouse at this specific time point. Speed was calculated as the distance between temporally adjacent positions multiplied by 15 (15-Hz recording). Freezing periods were sorted out if the area of the mouse body between temporally adjacent frames was less than 20 mm^2.

Audio data processing

Audio signal data was processed with custom scripts written in MATLAB R2015b (MathWorks). Each recorded WAV audio file was read and transformed into a spectrogram using fast Fourier transform with non-overlapping 0.4-ms time windows. To identify the time segments with ultrasonic vocalization signals, recordings were thresholded at a power spectral density (PSD) ≥-75 dB/Hz, and time segments with averaged PSD between 0–50 kHz higher than that between 50–120 kHz were removed. The duration of remaining time segments was calculated.

Statistical analysis

Numerical data were analyzed with custom scripts written in MATLAB R2015b (MathWorks). Statistical significance of the difference between 2 mean values was estimated with two-tailed, two-sample Student's t-test, except of DTI quantities and state-space behavioral comparison which were estimated with one-tailed, two-sample Student's t-test. Statistical significance of the difference between 2 median values (vocalization analysis; Figure 8F) was estimated using one-tailed Mann–Whitney U test.

To capture fine-scale behavioral details of location within the light-dark box and the elevated plus-maze (Figures 4 and 5), we computed T(x), the cumulative probability of finding position ≤x, for each individual (light traces) for all measured locations (a collection of locations from all mice for the statistics). We then show the average across the control group (bold blue trace) and the ParObsIso group (bold red trace). We compared the averages of each group with a two-tailed, two-sample Student's t-test and plot the resulting p-values, presented as -log(p), the negative logarithm of p-values. We also show the box plot (the minimum, lower quartile, median, upper quartile, and maximum) of -log(p) values collapsed across all measured locations. To capture the fine-scale behavioral details of speed, we followed a similar procedure as above, but with U(v), the cumulative distribution function of finding speed ≤v.

To estimate local likelihoods of caffeine-injected, foot-shocked, and non-treated behavior in the light-dark box or elevated plus-maze tests for any given 4-dimensional behavioral states described by the position, speed, velocity along the stressor axis, and acceleration strength, we trained a deterministic 3-layer feedforward network with hidden layer sizes of 26, 30, and 24 units, respectively, using log-sigmoid transfer functions. For pattern recognition, each network was trained by using the scaled conjugate gradient method to minimize cross-entropy to obtain reliable classifiers, with a random data division of 80% for training and 20% for testing. Training of updating weights and biases terminated when one of the following condition was matched: (1) reaching 1,000 iterations, (2) obtaining a perfect data fitting [i.e. the mean squared error (MSE) equaled to zero], (3) having the error rate continuously increasing for more than 6 epochs, (4) showing the gradient of MSE less than 10^{-7}, and (5) receiving the training gain larger than 10^{10}. The global likelihoods of a recorded mouse to be caffeine-injected-like, foot-shocked-like, and non-treated-like were calculated by taking the average of local likelihoods of each experimental type estimated by the corresponding trained network.

To evaluate the uncertainty of the percentage for each tail rattle count (Figure 10A), we created 10,000 bootstrapped data sets where each sample was randomly picked with replacement from the original data set. Each bootstrapped data set had the same sample size as the original data set. The standard error was taken as the standard deviation of the bootstrapped percentages for a tail rattle count. A similar procedure was carried out to evaluate the standard error of mean for the percentage of time spent in each behavior in the partner-revisiting test (Figures 10H and 11E), where each sample of the bootstrapped data sets was a set of the percentages of the three classified behaviors (partner concern, stranger concern, and non-social activity/sniffing at social targets) from a mouse record. Standard errors of means for other

results were estimated with the formula $\sigma/\sqrt{n}$, where σ is the sample standard deviation and n is the sample size.

Acknowledgments: We thank Tsuyoshi Koide (NIG, Japan), Aki Takahashi (University of Tsukuba), Teruhiro Okuyama (MIT), Charles Yokoyama (RIKEN BSI), Ai Koizumi (CiNet), and Tsai-Wen Chen (National Yang-Ming University) for comments, Tadashi Yamamoto (OIST) for sharing behavior testing setups, and Steven D. Aird (OIST) for editing the manuscript.

Competing interests: The authors declare no competing interests.

Funding: We acknowledge a JSPS KAKENHI Grant (JP 16J10077) by DC1 Student Research Fellowship to R.X.L. and OIST internal funding to B.K. The funders had no role in study design, data collection and interpretation, or the decision to submit the work for publication.

Author contributions: R.X.L. conceptualized the study, designed the research, performed experiments, analyzed data, interpreted results, wrote the original draft, and revised the article; G.J.S. advised on data analysis and revised the article; B.K. advised on research design and revised the article.

References:

Adams, R.E., Boscarino, J.A., 2006. Predictors of PTSD and Delayed PTSD After Disaster: The Impact of Exposure and Psychosocial Resources. J. Nerv. Ment. Dis. 194, 485–493. https://doi.org/10.1097/01.nmd.0000228503.95503.e9

Anderson, D.J., 2016. Circuit modules linking internal states and social behaviour in flies and mice. Nat. Rev. Neurosci. 17, 692–704. https://doi.org/10.1038/nrn.2016.125

Anderson, D.J., Adolphs, R., 2014. A framework for studying emotions across species. Cell 157, 187–200. https://doi.org/10.1016/j.cell.2014.03.003

Anderson, D.J., Perona, P., 2014. Toward a Science of Computational Ethology. Neuron 84, 18–31. https://doi.org/10.1016/j.neuron.2014.09.005

Andrews, B., Brewin, C.R., Philpott, R., Stewart, L., 2007. Delayed-Onset Posttraumatic Stress Disorder: A Systematic Review of the Evidence. Am. J. Psychiatry 164, 1319–1326. https://doi.org/10.1176/appi.ajp.2007.06091491

Arakawa, T., Tanave, A., Ikeuchi, S., Takahashi, A., Kakihara, S., Kimura, S., Sugimoto, H., Asada, N., Shiroishi, T., Tomihara, K., Tsuchiya, T., Koide, T., 2014. A male-specific QTL for social interaction behavior in mice mapped with automated pattern detection by

1064 a hidden Markov model incorporated into newly developed freeware. J. Neurosci.
1065 Methods 234, 127–134. https://doi.org/10.1016/J.JNEUMETH.2014.04.012
1066 Archer, J., 1973. Tests for emotionality in rats and mice: A review. Anim. Behav. 21, 205–235.
1067 https://doi.org/10.1016/S0003-3472(73)80065-X
1068 Avesar, D., Gulledge, A.T., 2012. Selective serotonergic excitation of callosal projection
1069 neurons. Front. Neural Circuits 6, 12. https://doi.org/10.3389/fncir.2012.00012
1070 Balogh, S.A., Radcliffe, R.A., Logue, S.F., Wehner, J.M., 2002. Contextual and cued fear
1071 conditioning in C57BL/6J and DBA/2J mice: Context discrimination and the effects of
1072 retention interval. Behav. Neurosci. 116, 947–957. https://doi.org/10.1037/0735-
1073 7044.116.6.947
1074 Basser, P.J., Mattiello, J., LeBihan, D., 1994. MR diffusion tensor spectroscopy and imaging.
1075 Biophys. J. 66, 259–267. https://doi.org/10.1016/S0006-3495(94)80775-1
1076 Berton, O., McClung, C.A., Dileone, R.J., Krishnan, V., Renthal, W., Russo, S.J., Graham, D.,
1077 Tsankova, N.M., Bolanos, C.A., Rios, M., Monteggia, L.M., Self, D.W., Nestler, E.J.,
1078 2006. Essential role of BDNF in the mesolimbic dopamine pathway in social defeat stress.
1079 Science 311, 864–8. https://doi.org/10.1126/science.1120972
1080 Bolton, S., Robinson, O.J., 2017. The impact of threat of shock-induced anxiety on memory
1081 encoding and retrieval. Learn. Mem. 24, 532–542. https://doi.org/10.1101/lm.045187.117
1082 Borsini, F., Podhorna, J., Marazziti, D., 2002. Do animal models of anxiety predict anxiolytic-
1083 like effects of antidepressants? Psychopharmacology (Berl). 163, 121–141.
1084 https://doi.org/10.1007/s00213-002-1155-6
1085 Bremner, J.D., Mletzko, T., Welter, S., Quinn, S., Williams, C., Brummer, M., Siddiq, S., Reed,
1086 L., Heim, C.M., Nemeroff, C.B., 2005. Effects of phenytoin on memory, cognition and
1087 brain structure in post-traumatic stress disorder: a pilot study. J. Psychopharmacol. 19,
1088 159–165. https://doi.org/10.1177/0269881105048996
1089 Bryant, R.A., Creamer, M., O'Donnell, M., Forbes, D., McFarlane, A.C., Silove, D., Hadzi-
1090 Pavlovic, D., 2017. Acute and Chronic Posttraumatic Stress Symptoms in the Emergence
1091 of Posttraumatic Stress Disorder. JAMA Psychiatry 74, 135.
1092 https://doi.org/10.1001/jamapsychiatry.2016.3470
1093 Bryant, R.A., O'Donnell, M.L., Creamer, M., McFarlane, A.C., Silove, D., 2013. A Multisite
1094 Analysis of the Fluctuating Course of Posttraumatic Stress Disorder. JAMA Psychiatry
1095 70, 839. https://doi.org/10.1001/jamapsychiatry.2013.1137
1096 Calhoon, G.G., Tye, K.M., 2015. Resolving the neural circuits of anxiety. Nat. Neurosci. 18,
1097 1394–1404. https://doi.org/10.1038/nn.4101

1098 Carobrez, A.P., Bertoglio, L.J., 2005. Ethological and temporal analyses of anxiety-like
1099 behavior: The elevated plus-maze model 20 years on. Neurosci. Biobehav. Rev. 29, 1193–
1100 1205. https://doi.org/10.1016/j.neubiorev.2005.04.017
1101 Chen, A., Shlapobersky, T., Schneidman, E., Shemesh, Y., Sztainberg, Y., Forkosh, O., 2013.
1102 High-order social interactions in groups of mice. Elife.
1103 https://doi.org/10.7554/elife.00759
1104 Cloninger, C.R., 1988. Anxiety and Theories of Emotion. Handb. Anxiety 2, 1–29.
1105 Cohen, S., Wills, T.A., 1985. Stress, Social Support, and the Buffering Hypothesis,
1106 Psychologkal Bulletin.
1107 Crawley, J., Goodwin, F.K., 1980. Preliminary report of a simple animal behavior model for
1108 the anxiolytic effects of benzodiazepines. Pharmacol. Biochem. Behav. 13, 167–170.
1109 https://doi.org/10.1016/0091-3057(80)90067-2
1110 Crusio, W.E., 2013. The genetics of exploratory behavior, in: Crusio, W.E., Sluyter, F., Gerlai,
1111 R.T., Pietropaolo, S. (Eds.), Behavioral Genetics of the Mouse. Cambridge University
1112 Press, Cambridge, pp. 148–154. https://doi.org/10.1017/CBO9781139541022.016
1113 Cryan, J.F., Holmes, A., 2005. The ascent of mouse: advances in modelling human depression
1114 and anxiety. Nat. Rev. Drug Discov. 4, 775–790. https://doi.org/10.1038/nrd1825
1115 Davis, M., 1989. Sensitization of the acoustic startle reflex by footshock. Behav. Neurosci. 103,
1116 495–503. https://doi.org/10.1037/0735-7044.103.3.495
1117 DeMorrow, S., DeMorrow, Sharon, 2018. Role of the Hypothalamic–Pituitary–Adrenal Axis
1118 in Health and Disease. Int. J. Mol. Sci. 19, 986. https://doi.org/10.3390/ijms19040986
1119 Dik, A., Saffari, R., Zhang, M., Zhang, W., 2018. Contradictory effects of erythropoietin on
1120 inhibitory synaptic transmission in left and right prelimbic cortex of mice. Neurobiol.
1121 Stress 9, 113–123. https://doi.org/10.1016/J.YNSTR.2018.08.008
1122 Diven, K., 1937. Certain Determinants in the Conditioning of Anxiety Reactions. J. Psychol.
1123 3, 291–308. https://doi.org/10.1080/00223980.1937.9917499
1124 Donaldson, G.P., Melanie Lee, S., Mazmanian, S.K., 2015. Gut biogeography of the bacterial
1125 microbiota. Nat. Publ. Gr. 14. https://doi.org/10.1038/nrmicro3552
1126 DSM-5, 2013. Diagnostic and statistical manual of mental disorders (DSM-5). Am. Psychiatr.
1127 Assoc. 947. https://doi.org/10.1176/appi.books.9780890425596
1128 DSM-III, 1980. Diagnostic and statistical manual of mental disorders (DSM-III). Am.
1129 Psychiatr. Assoc.
1130 Ehlers, A., Clark, D.M., 2000. A cognitive model of posttraumatic stress disorder. Behav. Res.
1131 Ther. 38, 319–345. https://doi.org/10.1016/S0005-7967(99)00123-0

1132 Engin, E., Treit, D., 2008. The effects of intra-cerebral drug infusions on animals'
1133 unconditioned fear reactions: A systematic review. Prog. Neuro-Psychopharmacology
1134 Biol. Psychiatry 32, 1399–1419. https://doi.org/10.1016/j.pnpbp.2008.03.020
1135 Ennaceur, A., 2014. Tests of unconditioned anxiety — Pitfalls and disappointments. Physiol.
1136 Behav. 135, 55–71. https://doi.org/10.1016/j.physbeh.2014.05.032
1137 Funamizu, A., Kuhn, B., Doya, K., 2016. Neural substrate of dynamic Bayesian inference in
1138 the cerebral cortex. Nat. Neurosci. 19, 1682–1689. https://doi.org/10.1038/nn.4390
1139 Garcia, A.M.B., Martinez, R.C.R., Morato, S., 2008. Preference for the light compartment of a
1140 light/dark cage does not affect rat exploratory behavior in the elevated plus-maze. Psychol.
1141 & Neurosci. 1, 73–80. https://doi.org/10.1590/s1983-32882008000100012
1142 Gilbertson, M.W., Shenton, M.E., Ciszewski, A., Kasai, K., Lasko, N.B., Orr, S.P., Pitman,
1143 R.K., 2002. Smaller hippocampal volume predicts pathologic vulnerability to
1144 psychological trauma. Nat. Neurosci. 5, 1242–1247. https://doi.org/10.1038/nn958
1145 Goto, T., Kubota, Y., Tanaka, Y., Iio, W., Moriya, N., Toyoda, A., 2014. Subchronic and mild
1146 social defeat stress accelerates food intake and body weight gain with polydipsia-like
1147 features in mice. Behav. Brain Res. 270, 339–348.
1148 https://doi.org/10.1016/J.BBR.2014.05.040
1149 Grupe, D.W., Nitschke, J.B., 2013. Uncertainty and anticipation in anxiety: an integrated
1150 neurobiological and psychological perspective. Nat. Rev. Neurosci. 14, 488–501.
1151 https://doi.org/10.1038/nrn3524
1152 Gulick, D., Gould, T.J., 2009. Effects of Ethanol and Caffeine on Behavior in C57BL/6 Mice
1153 in the Plus-Maze Discriminative Avoidance Task. Behav. Neurosci. 123, 1271–1278.
1154 https://doi.org/10.1037/a0017610
1155 Hall, C., Ballachey, E.L., 1932. A study of the rat's behavior in a field. A contribution to
1156 method in comparative psychology. Univ. Calif. Publ. Psychol. 1–12.
1157 Harvey, M.R., 1996. An ecological view of psychological trauma and trauma recovery. J.
1158 Trauma. Stress 9, 3–23. https://doi.org/10.1002/jts.2490090103
1159 Hascoët, M., Bourin, M., Nic Dhonnchadha, B.Á., 2001. The mouse ligth-dark paradigm: A
1160 review. Prog. Neuro-Psychopharmacology Biol. Psychiatry 25, 141–166.
1161 https://doi.org/10.1016/S0278-5846(00)00151-2
1162 Hayes, J.P., VanElzakker, M.B., Shin, L.M., 2012. Emotion and cognition interactions in PTSD:
1163 a review of neurocognitive and neuroimaging studies. Front. Integr. Neurosci. 6, 89.
1164 https://doi.org/10.3389/fnint.2012.00089

1165 Henriques-Alves, A.M., Queiroz, C.M., 2016. Ethological Evaluation of the Effects of Social
1166 Defeat Stress in Mice: Beyond the Social Interaction Ratio. Front. Behav. Neurosci. 9,
1167 364. https://doi.org/10.3389/fnbeh.2015.00364
1168 Hetrick, S.E., Purcell, R., Garner, B., Parslow, R., 2010. Combined pharmacotherapy and
1169 psychological therapies for post traumatic stress disorder (PTSD). Cochrane Database
1170 Syst. Rev. https://doi.org/10.1002/14651858.CD007316.pub2
1171 Houston, F.P., Stevenson, G.D., McNaughton, B.L., Barnes, C.A., 1999. Effects of age on the
1172 generalization and incubation of memory in the F344 rat. Learn. Mem. 6, 111–9.
1173 https://doi.org/10.1101/LM.6.2.111
1174 Hrabe, J., Kaur, G., Guilfoyle, D.N., 2007. Principles and limitations of NMR diffusion
1175 measurements. J. Med. Phys. 32, 34–42. https://doi.org/10.4103/0971-6203.31148
1176 Kaouane, N., Porte, Y., Vallée, M., Brayda-Bruno, L., Mons, N., Calandreau, L., Marighetto,
1177 A., Piazza, P.V., Desmedt, A., 2012. Glucocorticoids can induce PTSD-like memory
1178 impairments in mice. Science 335, 1510–3. https://doi.org/10.1126/science.1207615
1179 Kim, S., Mátyás, F., Lee, S., Acsády, L., Shin, H.-S., 2012. Lateralization of observational fear
1180 learning at the cortical but not thalamic level in mice. Proc. Natl. Acad. Sci. U. S. A. 109,
1181 15497–501. https://doi.org/10.1073/pnas.1213903109
1182 Knox, D., George, S.A., Fitzpatrick, C.J., Rabinak, C.A., Maren, S., Liberzon, I., 2012. Single
1183 prolonged stress disrupts retention of extinguished fear in rats. Learn. Mem. 19, 43–9.
1184 https://doi.org/10.1101/lm.024356.111
1185 Ko, J., 2017. Neuroanatomical Substrates of Rodent Social Behavior: The Medial Prefrontal
1186 Cortex and Its Projection Patterns. Front. Neural Circuits 11, 41.
1187 https://doi.org/10.3389/fncir.2017.00041
1188 Kohl, J., Babayan, B.M., Rubinstein, N.D., Autry, A.E., Marin-Rodriguez, B., Kapoor, V.,
1189 Miyamishi, K., Zweifel, L.S., Luo, L., Uchida, N., Dulac, C., 2018. Functional circuit
1190 architecture underlying parental behaviour. Nature 556, 326–331.
1191 https://doi.org/10.1038/s41586-018-0027-0
1192 Krishnan, V., Han, M.-H., Graham, D.L., Berton, O., Renthal, W., Russo, S.J., Laplant, Q.,
1193 Graham, A., Lutter, M., Lagace, D.C., Ghose, S., Reister, R., Tannous, P., Green, T.A.,
1194 Neve, R.L., Chakravarty, S., Kumar, A., Eisch, A.J., Self, D.W., Lee, F.S., Tamminga,
1195 C.A., Cooper, D.C., Gershenfeld, H.K., Nestler, E.J., 2007. Molecular adaptations
1196 underlying susceptibility and resistance to social defeat in brain reward regions. Cell 131,
1197 391–404. https://doi.org/10.1016/j.cell.2007.09.018

1198 Kulesskaya, N., Voikar, V., 2014. Assessment of mouse anxiety-like behavior in the light–dark
1199 box and open-field arena: Role of equipment and procedure. Physiol. Behav. 133, 30–38.
1200 https://doi.org/10.1016/J.PHYSBEH.2014.05.006
1201 Kumar, V., Bhat, Z.A., Kumar, D., 2013. Animal models of anxiety: A comprehensive review.
1202 J. Pharmacol. Toxicol. Methods 68, 175–183.
1203 https://doi.org/10.1016/J.VASCN.2013.05.003
1204 Larkum, M., 2013. A cellular mechanism for cortical associations: an organizing principle for
1205 the cerebral cortex. Trends Neurosci. 36, 141–151.
1206 https://doi.org/10.1016/J.TINS.2012.11.006
1207 Lee, E., Hong, J., Park, Y.-G., Chae, S., Kim, Y., Kim, D., 2015. Left brain cortical activity
1208 modulates stress effects on social behavior. Sci. Rep. 5, 13342.
1209 https://doi.org/10.1038/srep13342
1210 Lee, R.X., Huang, J.-J., Huang, C., Tsai, M.-L., Yen, C.-T., 2015. Plasticity of cerebellar
1211 Purkinje cells in behavioral training of body balance control. Front. Syst. Neurosci. 9, 1–
1212 15. https://doi.org/10.3389/fnsys.2015.00113
1213 Lee, R.X., Huang, J.J., Huang, C., Tsai, M.L., Yen, C.T., 2014. Collateral projections from
1214 vestibular nuclear and inferior olivary neurons to lobules I/II and IX/X of the rat cerebellar
1215 vermis: A double retrograde labeling study. Eur. J. Neurosci. 40, 2811–2821.
1216 https://doi.org/10.1111/ejn.12648
1217 Marlin, B.J., Froemke, R.C., 2017. Oxytocin modulation of neural circuits for social behavior.
1218 Dev. Neurobiol. 77, 169–189. https://doi.org/10.1002/dneu.22452
1219 Marlin, B.J., Mitre, M., D'amour, J.A., Chao, M. V., Froemke, R.C., 2015. Oxytocin enables
1220 maternal behaviour by balancing cortical inhibition. Nature 520, 499–504.
1221 https://doi.org/10.1038/nature14402
1222 Mataix-Cols, D., Fernández de la Cruz, L., Monzani, B., Rosenfield, D., Andersson, E., Pérez-
1223 Vigil, A., Frumento, P., de Kleine, R.A., Difede, J., Dunlop, B.W., Farrell, L.J., Geller,
1224 D., Gerardi, M., Guastella, A.J., Hofmann, S.G., Hendriks, G.-J., Kushner, M.G., Lee,
1225 F.S., Lenze, E.J., Levinson, C.A., McConnell, H., Otto, M.W., Plag, J., Pollack, M.H.,
1226 Ressler, K.J., Rodebaugh, T.L., Rothbaum, B.O., Scheeringa, M.S., Siewert-Siegmund,
1227 A., Smits, J.A.J., Storch, E.A., Ströhle, A., Tart, C.D., Tolin, D.F., van Minnen, A., Waters,
1228 A.M., Weems, C.F., Wilhelm, S., Wyka, K., Davis, M., Rück, C., Altemus, M., Anderson,
1229 P., Cukor, J., Finck, C., Geffken, G.R., Golfels, F., Goodman, W.K., Gutner, C., Heyman,
1230 I., Jovanovic, T., Lewin, A.B., McNamara, J.P., Murphy, T.K., Norrholm, S., Thuras, P.,
1231 2017. D-Cycloserine Augmentation of Exposure-Based Cognitive Behavior Therapy for

Anxiety, Obsessive-Compulsive, and Posttraumatic Stress Disorders. JAMA Psychiatry 74, 501. https://doi.org/10.1001/jamapsychiatry.2016.3955

Matias, S., Lottem, E., Dugué, G.P., Mainen, Z.F., 2017. Activity patterns of serotonin neurons underlying cognitive flexibility. Elife 6, e20552. https://doi.org/10.7554/eLife.20552

McAllister DE, M.W., 1967. Incubation of fear: An examination of the concept. J Exp Res Personal. 2, 180–190.

McFarlane, A.C., 2010. The long-term costs of traumatic stress: intertwined physical and psychological consequences. World Psychiatry 9, 3–10. https://doi.org/10.1002/j.2051-5545.2010.tb00254.x

McHugh, P.R., Treisman, G., 2007. PTSD: A problematic diagnostic category. J. Anxiety Disord. 21, 211–222. https://doi.org/10.1016/J.JANXDIS.2006.09.003

McIntyre, D.C., 2006. The Kindling Phenomenon. Model. Seizures Epilepsy 351–363. https://doi.org/10.1016/B978-012088554-1/50030-X

McIntyre, D.C., Kelly, M.E., 2006. The Parahippocampal Cortices and Kindling. Ann. N. Y. Acad. Sci. 911, 343–354. https://doi.org/10.1111/j.1749-6632.2000.tb06736.x

Miczek, K.A., O'Donnell, J.M., 1978. Intruder-evoked aggression in isolated and nonisolated mice: Effects of psychomotor stimulants and l-Dopa. Psychopharmacology (Berl). 57, 47–55. https://doi.org/10.1007/BF00426957

Mori, S. (Susumu), 2007. Introduction to diffusion tensor imaging. Elsevier.

Murugan, M., Jang, H.J., Park, M., Miller, E.M., Cox, J., Taliaferro, J.P., Parker, N.F., Bhave, V., Hur, H., Liang, Y., Nectow, A.R., Pillow, J.W., Witten, I.B., 2017. Combined Social and Spatial Coding in a Descending Projection from the Prefrontal Cortex. Cell 171, 1663-1677.e16. https://doi.org/10.1016/j.cell.2017.11.002

Nadler, J.J., Moy, S.S., Dold, G., Simmons, N., Perez, A., Young, N.B., Barbaro, R.P., Piven, J., Magnuson, T.R., Crawley, J.N., Crawley, J.N., 2004. Automated apparatus for quantitation of social approach behaviors in mice. Genes, Brain Behav. 3, 303–314. https://doi.org/10.1111/j.1601-183X.2004.00071.x

Nath, T., Mathis, A., Chen, A.C., Patel, A., Bethge, M., Mathis, M.W., 2019. Using DeepLabCut for 3D markerless pose estimation across species and behaviors. Nat. Protoc. 1. https://doi.org/10.1038/s41596-019-0176-0

Otabi, H., Goto, T., Okayama, T., Kohari, D., Toyoda, A., 2017. The acute social defeat stress and nest-building test paradigm: A potential new method to screen drugs for depressive-like symptoms. Behav. Processes 135, 71–75. https://doi.org/10.1016/J.BEPROC.2016.12.003

Pai, A., Suris, A., North, C., Pai, A., Suris, A.M., North, C.S., 2017. Posttraumatic Stress Disorder in the DSM-5: Controversy, Change, and Conceptual Considerations. Behav. Sci. (Basel). 7, 7. https://doi.org/10.3390/bs7010007

Pamplona, F.A., Henes, K., Micale, V., Mauch, C.P., Takahashi, R.N., Wotjak, C.T., 2011. Prolonged fear incubation leads to generalized avoidance behavior in mice. J. Psychiatr. Res. 45, 354–360. https://doi.org/10.1016/J.JPSYCHIRES.2010.06.015

Patki, G., Solanki, N., Salim, S., 2014. Witnessing traumatic events causes severe behavioral impairments in rats. Int. J. Neuropsychopharmacol. 17, 2017–2029. https://doi.org/10.1017/S1461145714000923

Pavić, L., Gregurek, R., Radoš, M., Brkljačić, B., Brajković, L., Šimetin-Pavić, I., Ivanac, G., Pavliša, G., Kalousek, V., 2007. Smaller right hippocampus in war veterans with posttraumatic stress disorder. Psychiatry Res. Neuroimaging 154, 191–198. https://doi.org/10.1016/J.PSCYCHRESNS.2006.08.005

Pellow, S., Chopin, P., File, S.E., Briley, M., 1985. Validation of open : closed arm entries in an elevated plus-maze as a measure of anxiety in the rat. J. Neurosci. Methods 14, 149–167. https://doi.org/10.1016/0165-0270(85)90031-7

Philbert, J., Pichat, P., Beeské, S., Decobert, M., Belzung, C., Griebel, G., 2011. Acute inescapable stress exposure induces long-term sleep disturbances and avoidance behavior: A mouse model of post-traumatic stress disorder (PTSD). Behav. Brain Res. 221, 149–154. https://doi.org/10.1016/J.BBR.2011.02.039

Poulos, A.M., Reger, M., Mehta, N., Zhuravka, I., Sterlace, S.S., Gannam, C., Hovda, D.A., Giza, C.C., Fanselow, M.S., 2014. Amnesia for early life stress does not preclude the adult development of posttraumatic stress disorder symptoms in rats. Biol. Psychiatry 76, 306–14. https://doi.org/10.1016/j.biopsych.2013.10.007

Ramos, A., 2008. Animal models of anxiety: do I need multiple tests? Trends Pharmacol. Sci. 29, 493–498. https://doi.org/10.1016/J.TIPS.2008.07.005

Ramos, A., Pereira, E., Martins, G.C., Wehrmeister, T.D., Izídio, G.S., 2008. Integrating the open field, elevated plus maze and light/dark box to assess different types of emotional behaviors in one single trial. Behav. Brain Res. 193, 277–288. https://doi.org/10.1016/J.BBR.2008.06.007

Rau, V., DeCola, J.P., Fanselow, M.S., 2005. Stress-induced enhancement of fear learning: An animal model of posttraumatic stress disorder. Neurosci. Biobehav. Rev. 29, 1207–1223. https://doi.org/10.1016/J.NEUBIOREV.2005.04.010

1299 Remedios, R., Kennedy, A., Zelikowsky, M., Grewe, B.F., Schnitzer, M.J., Anderson, D.J.,
1300 2017. Social behaviour shapes hypothalamic neural ensemble representations of
1301 conspecific sex. Nature 550, 388–392. https://doi.org/10.1038/nature23885
1302 Roome, C.J., Kuhn, B., 2018. Simultaneous dendritic voltage and calcium imaging and somatic
1303 recording from Purkinje neurons in awake mice. Nat. Commun. 9, 3388.
1304 https://doi.org/10.1038/s41467-018-05900-3
1305 Scherer, A., Boecker, M., Pawelzik, M., Gauggel, S., Forkmann, T., 2017. Emotion
1306 suppression, not reappraisal, predicts psychotherapy outcome. Psychother. Res. 27, 143–
1307 153. https://doi.org/10.1080/10503307.2015.1080875
1308 Schnyder, U., Cloitre, M., 2015. Evidence based treatments for trauma-related psychological
1309 disorders : a practical guide for clinicians.
1310 Shin, L.M., Rauch, S.L., Pitman, R.K., 2006. Amygdala, Medial Prefrontal Cortex, and
1311 Hippocampal Function in PTSD. Ann. N. Y. Acad. Sci. 1071, 67–79.
1312 https://doi.org/10.1196/annals.1364.007
1313 Sial, O.K., Warren, B.L., Alcantara, L.F., Parise, E.M., Bolaños-Guzmán, C.A., 2016.
1314 Vicarious social defeat stress: Bridging the gap between physical and emotional stress. J.
1315 Neurosci. Methods 258, 94–103. https://doi.org/10.1016/J.JNEUMETH.2015.10.012
1316 Siegmund, A., Wotjak, C.T., 2006. Toward an Animal Model of Posttraumatic Stress Disorder.
1317 Ann. N. Y. Acad. Sci. 1071, 324–334. https://doi.org/10.1196/annals.1364.025
1318 Sillivan, S.E., Joseph, N.F., Jamieson, S., King, M.L., Chévere-Torres, I., Fuentes, I.,
1319 Shumyatsky, G.P., Brantley, A.F., Rumbaugh, G., Miller, C.A., 2017. Susceptibility and
1320 Resilience to Posttraumatic Stress Disorder–like Behaviors in Inbred Mice. Biol.
1321 Psychiatry 82, 924–933. https://doi.org/10.1016/J.BIOPSYCH.2017.06.030
1322 Stephens, E.K., Avesar, D., Gulledge, A.T., 2014. Activity-dependent serotonergic excitation
1323 of callosal projection neurons in the mouse prefrontal cortex. Front. Neural Circuits 8, 97.
1324 https://doi.org/10.3389/fncir.2014.00097
1325 Suarez, S.D., Gallup, G.G., 1981. An ethological analysis of open-field behavior in rats and
1326 mice. Learn. Motiv. 12, 342–363. https://doi.org/10.1016/0023-9690(81)90013-8
1327 Sullivan, R.M., Gratton, A., 1998. Relationships between stress-induced increases in medial
1328 prefrontal cortical dopamine and plasma corticosterone levels in rats: role of cerebral
1329 laterality. Neuroscience 83, 81–91. https://doi.org/10.1016/S0306-4522(97)00370-9
1330 Takahashi, A., Lee, R.X., Iwasato, T., Itohara, S., Arima, H., Bettler, B., Miczek, K.A., Koide,
1331 T., 2015. Glutamate input in the dorsal raphe nucleus as a determinant of escalated
1332 aggression in male mice. J. Neurosci. 35, 6452–63.
1333 https://doi.org/10.1523/JNEUROSCI.2450-14.2015

1334 Tononi, G., Boly, M., Massimini, M., Koch, C., 2016. Integrated information theory: from
1335 consciousness to its physical substrate. Nat. Rev. Neurosci. 17, 450–461.
1336 https://doi.org/10.1038/nrn.2016.44
1337 Tovote, P., Fadok, J.P., Lüthi, A., 2015. Neuronal circuits for fear and anxiety. Nat. Rev.
1338 Neurosci. 16, 317–331. https://doi.org/10.1038/nrn3945
1339 Tsuda, M.C., Ogawa, S., 2012. Long-Lasting Consequences of Neonatal Maternal Separation
1340 on Social Behaviors in Ovariectomized Female Mice. PLoS One 7, e33028.
1341 https://doi.org/10.1371/journal.pone.0033028
1342 Tsuda, M.C., Yeung, H.-M., Kuo, J., Usdin, T.B., 2015. Incubation of Fear Is Regulated by
1343 TIP39 Peptide Signaling in the Medial Nucleus of the Amygdala. J. Neurosci. 35, 12152–
1344 61. https://doi.org/10.1523/JNEUROSCI.1736-15.2015
1345 Vasconcelos, M., Hollis, K., Nowbahari, E., Kacelnik, A., 2012. Pro-sociality without empathy.
1346 Biol. Lett. 8, 910–912. https://doi.org/10.1098/rsbl.2012.0554
1347 Walf, A.A., Frye, C.A., 2007. The use of the elevated plus maze as an assay of anxiety-related
1348 behavior in rodents. Nat. Protoc. 2, 322–328. https://doi.org/10.1038/nprot.2007.44
1349 Walton, J.L., Cuccurullo, L.-A.J., Raines, A.M., Vidaurri, D.N., Allan, N.P., Maieritsch, K.P.,
1350 Franklin, C.L., 2017. Sometimes Less is More: Establishing the Core Symptoms of PTSD.
1351 J. Trauma. Stress 30, 254–258. https://doi.org/10.1002/jts.22185
1352 Warren, B.L., Vialou, V.F., Iñiguez, S.D., Alcantara, L.F., Wright, K.N., Feng, J., Kennedy,
1353 P.J., LaPlant, Q., Shen, L., Nestler, E.J., Bolaños-Guzmán, C.A., 2013. Neurobiological
1354 Sequelae of Witnessing Stressful Events in Adult Mice. Biol. Psychiatry 73, 7–14.
1355 https://doi.org/10.1016/J.BIOPSYCH.2012.06.006
1356 Wu, L., Meng, J., Shen, Q., Zhang, Y., Pan, S., Chen, Z., Zhu, L.-Q., Lu, Y., Huang, Y., Zhang,
1357 G., 2017. Caffeine inhibits hypothalamic A1R to excite oxytocin neuron and ameliorate
1358 dietary obesity in mice. Nat. Commun. 8, 15904. https://doi.org/10.1038/ncomms15904
1359 Zelikowsky, M., Hui, M., Karigo, T., Choe, A., Yang, B., Blanco, M.R., Beadle, K., Gradinaru,
1360 V., Deverman, B.E., Anderson, D.J., 2018. The Neuropeptide Tac2 Controls a Distributed
1361 Brain State Induced by Chronic Social Isolation Stress. Cell 173, 1265-1279.e19.
1362 https://doi.org/10.1016/J.CELL.2018.03.037
1363 Zoladz, P.R., Diamond, D.M., 2013. Current status on behavioral and biological markers of
1364 PTSD: A search for clarity in a conflicting literature. Neurosci. Biobehav. Rev. 37, 860–
1365 895. https://doi.org/10.1016/J.NEUBIOREV.2013.03.024
1366

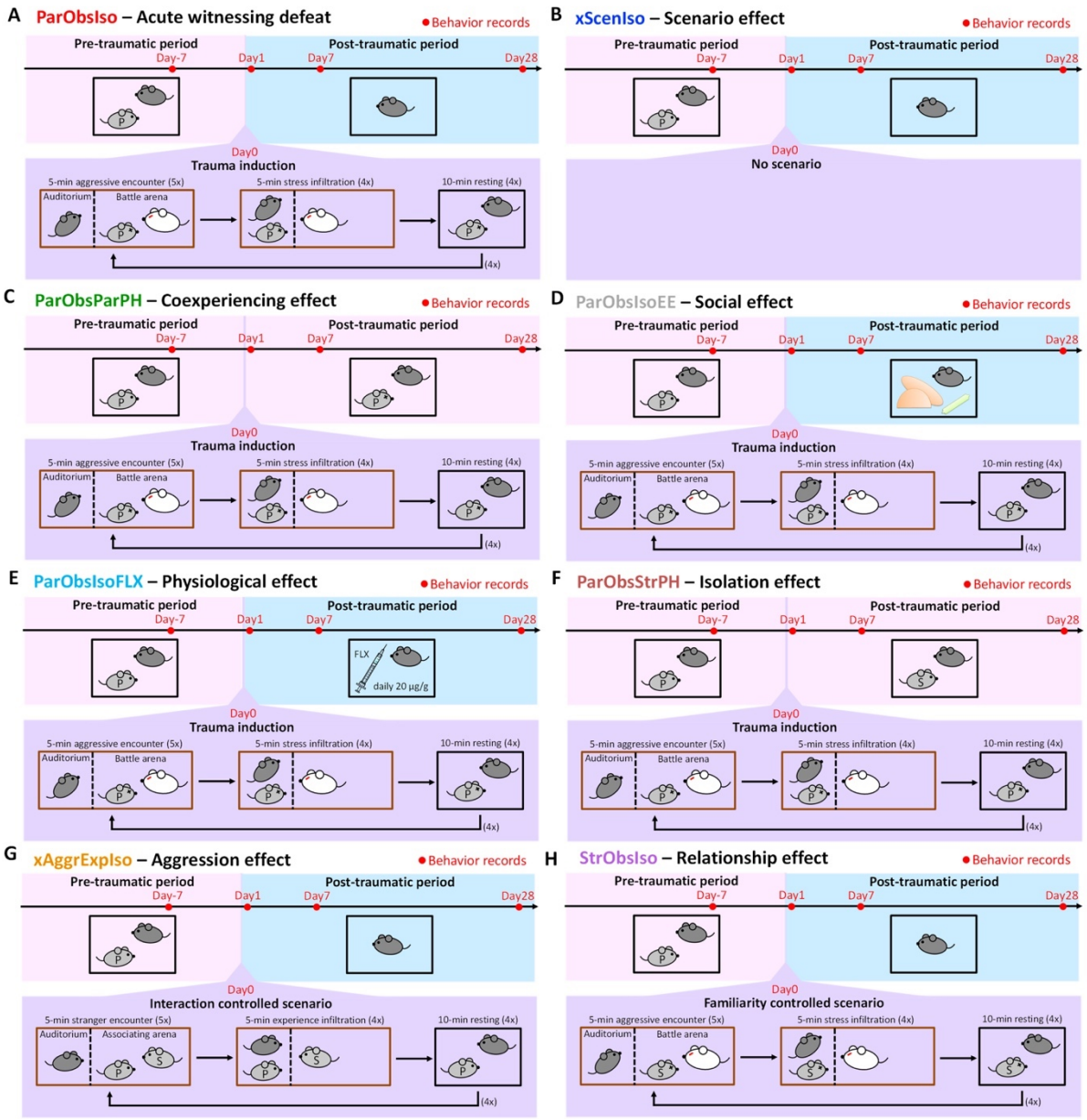

Figure 1. Paradigm inducing PTSD-like behavior in mice and seven control paradigms. (A) Paradigm with acute psychosocial trauma induction in mice. Focal mouse [dark gray; Partner-Observing-Isolated (ParObsIso) mouse], partner mouse (light gray P), aggressor mouse (white), focal mouse's homecage (black), aggressor's homecage (brown), and wire-meshed divider (dashed line). **(B)** No-Scenario-Isolated (xScenIso) mice were separated without trauma induction and identified the scenario effect in the behavioral paradigm. **(C)** Partner-Observing-Partner-Pair-Housed (ParObsParPH) mice were pair-housed with their partners after trauma induction and identified the social transfer effect of co-experiencing trauma in the behavioral paradigm. **(D)** Partner-Observing-Isolated-Environment-Enriched (ParObsIsoEE) mice were provided with toys after trauma induction and identified the social rescue effect in the behavioral paradigm. **(E)** Partner-Observing-Isolated-Fluoxetine-treated

1379 (ParObsIsoFLX) mice were treated with fluoxetine after trauma induction and identified the
1380 pharmacological rescue effect in the behavioral paradigm. **(F)** Partner-Observing-Stranger-
1381 Pair-Housed (ParObsStrPH) mice were pair-housed with strangers after trauma induction and
1382 identified the isolation effect in the behavioral paradigm. **(G)** Non-Aggressor-Exposed-
1383 Isolated (xAggrExpIso) mice had experience of social interactions without witnessing stress
1384 from strangers and identified the aggression effect in the behavioral paradigm. **(H)** Stranger-
1385 Observing-Isolated (StrObsIso) mice had witnessing experience of trauma that happened to
1386 strangers, rather than to their pair-housed partners, and identified the relationship effect in the
1387 behavioral paradigm.

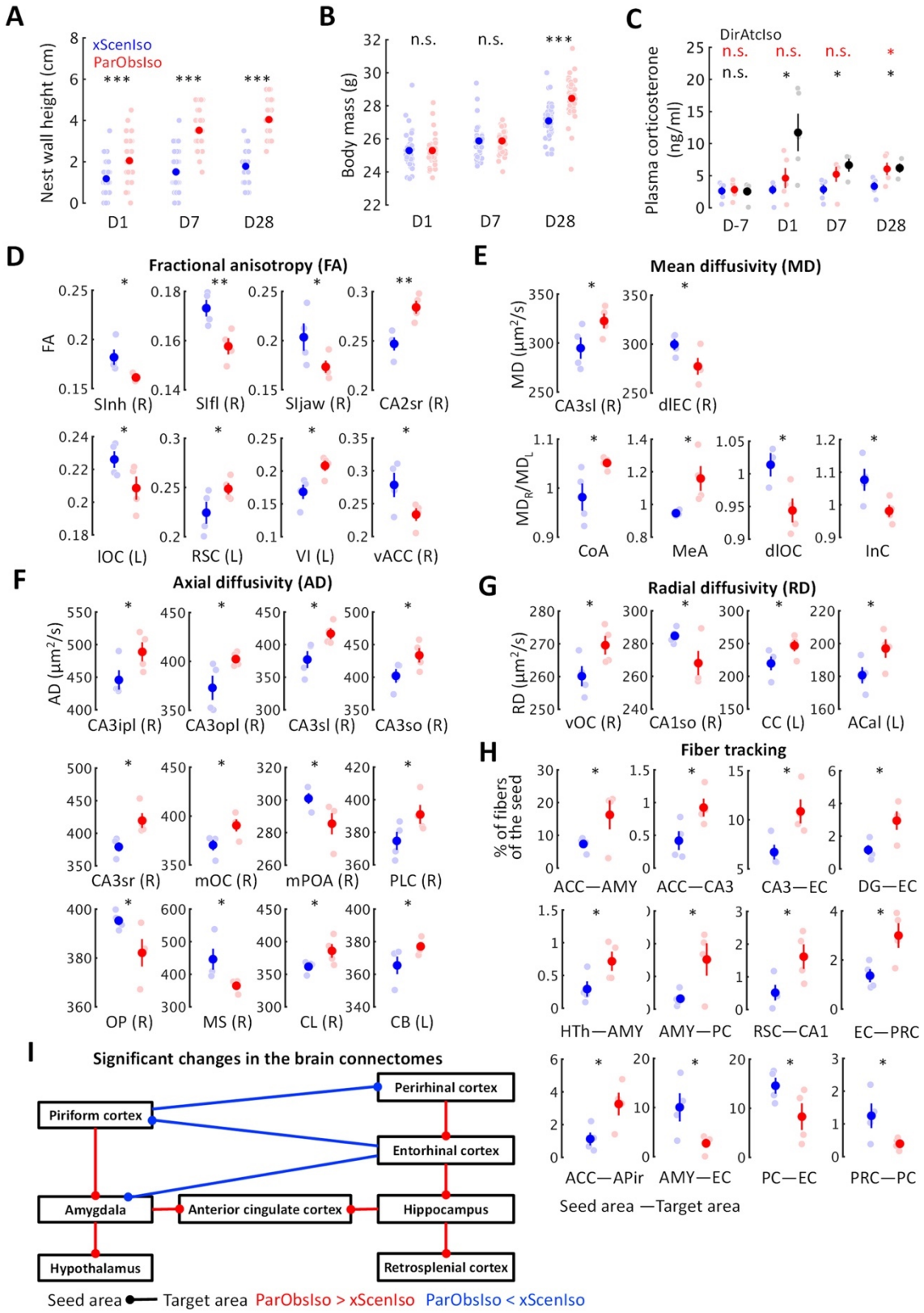

Figure 2. Long-term and delayed effects on multiple behaviors and physical conditions. **(A)** Nest wall heights show long-lasting significant differences after trauma induction. **(B)** Body mass shows a significant increase 28 days after trauma induction. **(C)** Baseline plasma

1392 corticosterone level increased after trauma induction for both ParObsIso mice and their partners,
1393 the DirAtcIso mice. **(D)** Fractional anisotropy (FA) of DTI-based water diffusivity suggests
1394 the changes of average microstructural integrity in multiple areas of the cerebral cortex. lOC,
1395 lateral orbital cortex; SInh, non-homunculus region of the primary sensory cortex; SIfl,
1396 forelimb region of the primary sensory cortex; SIjaw, jaw region of the primary sensory cortex;
1397 vACC, ventral region of the anterior cingulate cortex; CA2sr, stratum radiatum of the
1398 hippocampal cornu ammonis (CA) 2 area; RSC, the retrosplenial cortex; VI, the primary visual
1399 cortex; (R), the right area; (L), the left area. **(E)** DTI-based mean water diffusivity (MD)
1400 suggests the changes of membrane density in multiple areas of the entorhinal cortex-
1401 hippocampus system and the straitening of structural hemispheric specializations in the
1402 amygdala-insular cortex system. dlOC, dorsolateral orbital cortex; InC, the insular cortex; CoA,
1403 the cortical amygdalar nucleus; MeA, medial amygdalar nucleus; CA3sl, stratum lucidum of
1404 the hippocampal CA3 area; dlEC, dorsolateral entorhinal cortex. **(F)** DTI-based axial water
1405 diffusivity (AD) suggests the changes of neurite organization in multiple areas of the cerebral
1406 cortex and white matter mainly in the right hemisphere. OP, olfactory peduncle; PLC,
1407 prelimbic cortex; mOC, medial orbital cortex; CL, claustrum; MS, medial septal complex;
1408 mPOA, medial preoptic area; CB, cingulum bundle; CA3sr, stratum radiatum of the
1409 hippocampal CA3 area; CA3sl, stratum lucidum of the hippocampal CA3 area;CA3so, stratum
1410 oriens of the hippocampal CA3 area; CA3ipl, inner pyramidal layer of the hippocampal CA3
1411 area; CA3opl, outer pyramidal layer of the hippocampal CA3 area. **(G)** DTI-based radial water
1412 diffusivity (RD) suggests the changes of myelination in multiple areas of the cerebral cortex in
1413 the right hemisphere and the white matter in the left hemisphere. vOC, ventral orbital cortex;
1414 ACal, anterior limb of the anterior commissure; CC, corpus callosum; CA1so, stratum oriens
1415 of the hippocampal CA1 area. **(H)** DTI-based network-wise fiber tracking reveals specific
1416 chronic changes of structural connectivity in the brain. AMY, the amygdala; HTh, the
1417 hypothalamus; DG, the hippocampal dentate gyrus; PC, the piriform cortex; PRC, the
1418 perirhinal cortex; APir, the amygdalopiriform transition area. Note that the brain regions were
1419 in the right brain hemisphere. **(I)** Trauma-induced structural changes of the underlying brain
1420 connectome revealed a network enhancement centered at the anterior cingulate cortex. Error
1421 bars indicate standard errors of the means; n.s., $p \geq 0.05$; *, $0.01 \leq p < 0.05$; ***, $p < 0.001$; two-
1422 sample Student's t-test.

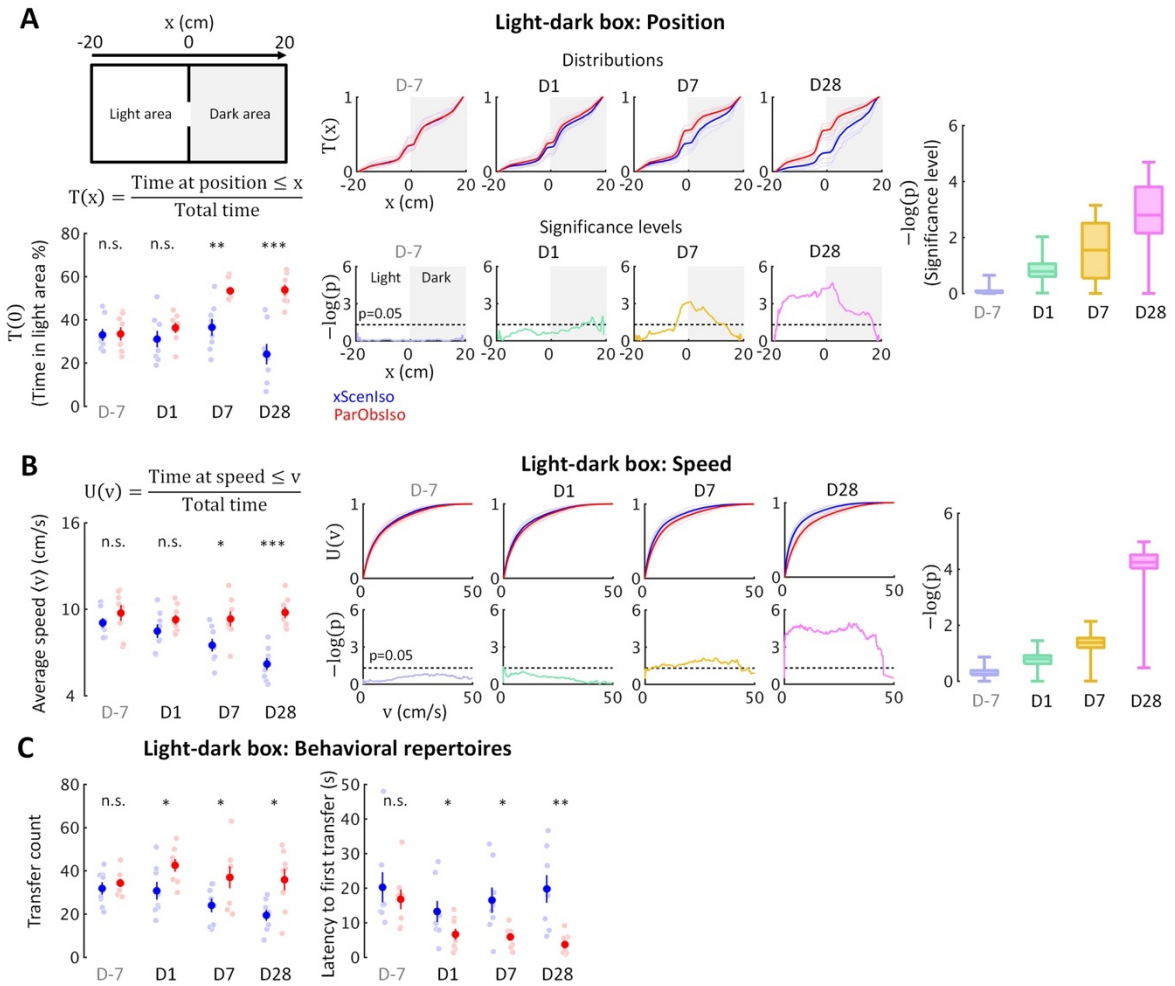

Figure 3. Fine-scale behavioral analysis in light-dark box test detects the gradually developing process of the behavioral difference. (A) Light-dark box test quantified through the cumulative position probability T(x) along the light-dark axis (left; total time = 300 s). On average, ParObsIso mice (red) spent more time in the light area than xScenIso mice (blue) during the late post-traumatic period [T(0), bottom-left]. Spatially fine-scale behavioral analysis reveals significant differences between ParObsIso and xScenIso populations already in the early post-traumatic period (middle). For each position, we compute the mean T(x) across the xScenIso and ParObsIso populations and compute statistical significance through a two-population Student's t-test. These differences gradually increased, as evidenced by significance distributions collapsed across all positions (right; box plots show the minima, lower quartiles, medians, upper quartiles, and maxima). **(B)** We similarly quantified speed using the fine-scale cumulative distribution U(v)of having speed ≤v and we show the statistical analysis of population differences in U(v). Cumulative distribution functions of locomotion speed (U(v) of having speed ≤v) and corresponding significance distributions provide an additional independent behavioral index that showed a gradually increasing differences of

1439 higher speed in ParObsIso mice. **(C)** Higher transfer counts and shorter latency to the first
1440 transfers in ParObsIso mice suggest their higher activity and exploratory motivation,
1441 respectively.

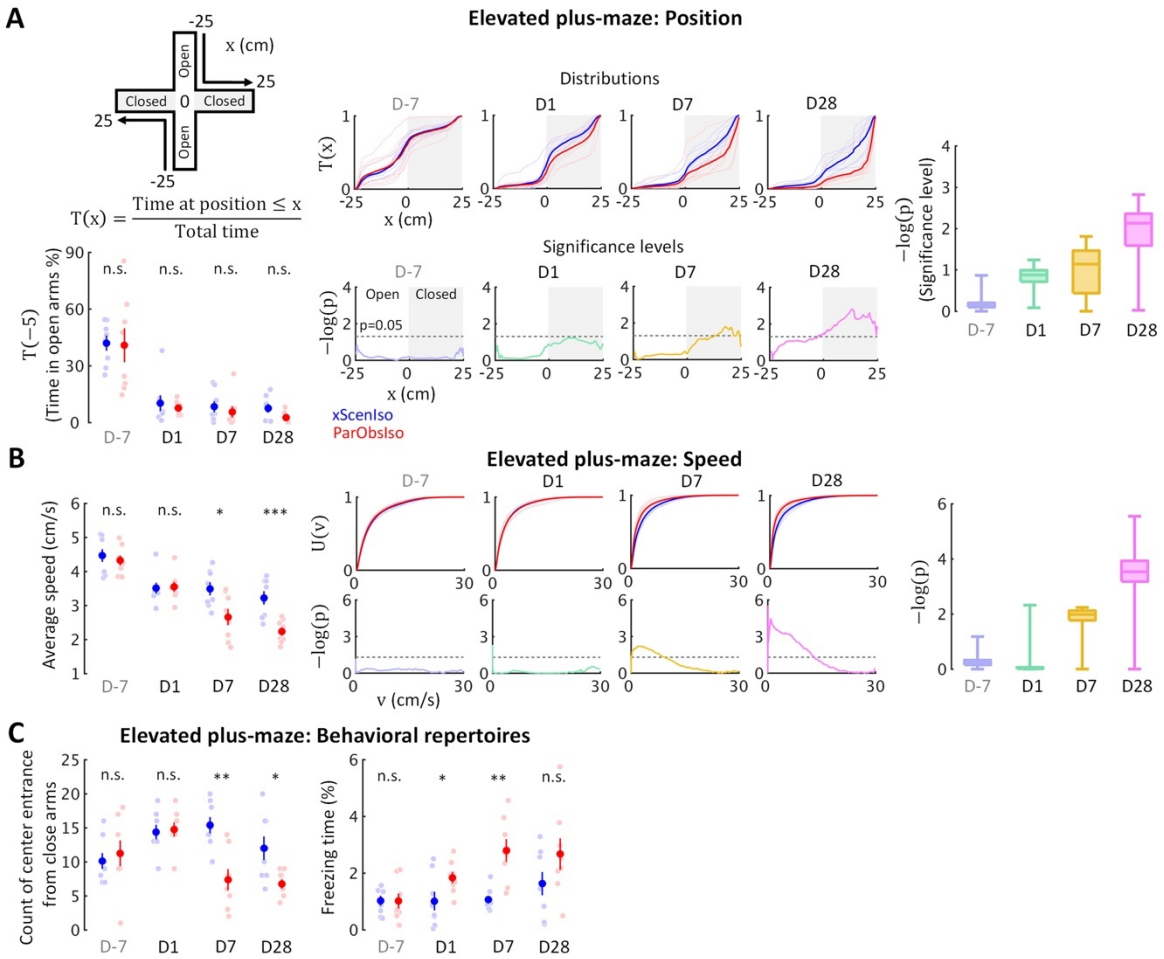

Figure 4. Behavioral testing in the elevated plus-maze demonstrates that stress incubation of anxiety caused the observed differences. (A) ParObsIso and xScenIso mice did not differ significantly in the time they spent in opened arms (total time = 300 s); however, spatial distributions show differences in preferred location between ParObsIso and xScenIso mice in the closed arms, which increased with time. **(B)** Cumulative distribution functions of locomotion speed and corresponding significance distributions show a gradually increasing differences of lower speeds in ParObsIso mice. **(C)** Less exploration from close arms to platform center and longer freezing time in ParObsIso mice suggest their stronger stress reactions.

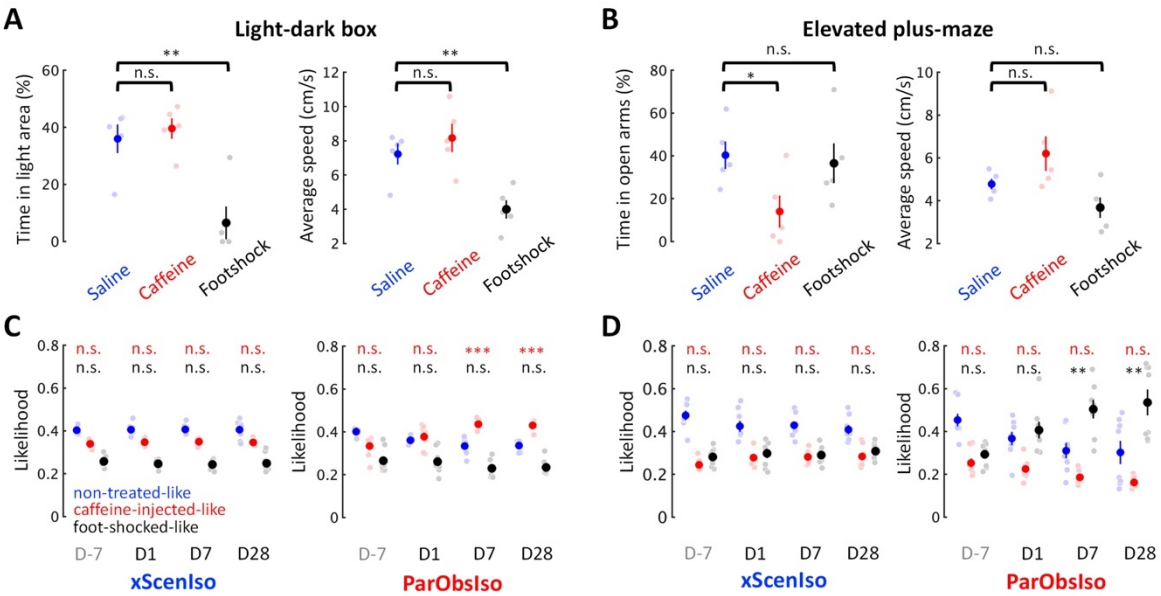

Figure 5. Comparison of behavioral characteristics in high-dimensional state-space indicates chronic somatic and cognitive anxiety developed in stress incubation. (A) Foot-shocked mice displayed less time spent in the light area and slower locomotion compared with the saline-injected and caffeine-injected mice in the light-dark box test. **(B)** Caffeine-injected mice displayed less time spent in the opened arms compared with the saline-injected and foot-shocked mice in the elevated plus-maze test. **(C)** In the light-dark box test, xScenIso mice stably showed non-treated-like behavioral characteristics after separated with its pair-housed partners, while ParObsIso mice increased their caffeine-injected-like behavioral characteristics in the corresponding period. **(D)** In the elevated plus-maze test, xScenIso mice kept showing highest likelihood of behavioral characteristics as non-treated-like after separated with its pair-housed partners, while ParObsIso mice increased their foot-shocked-like behavioral characteristics in the corresponding period. Note that comparison of behavioral characteristics in high-dimensional state-space was tested by one-tailed, two-sample Student's t-test.

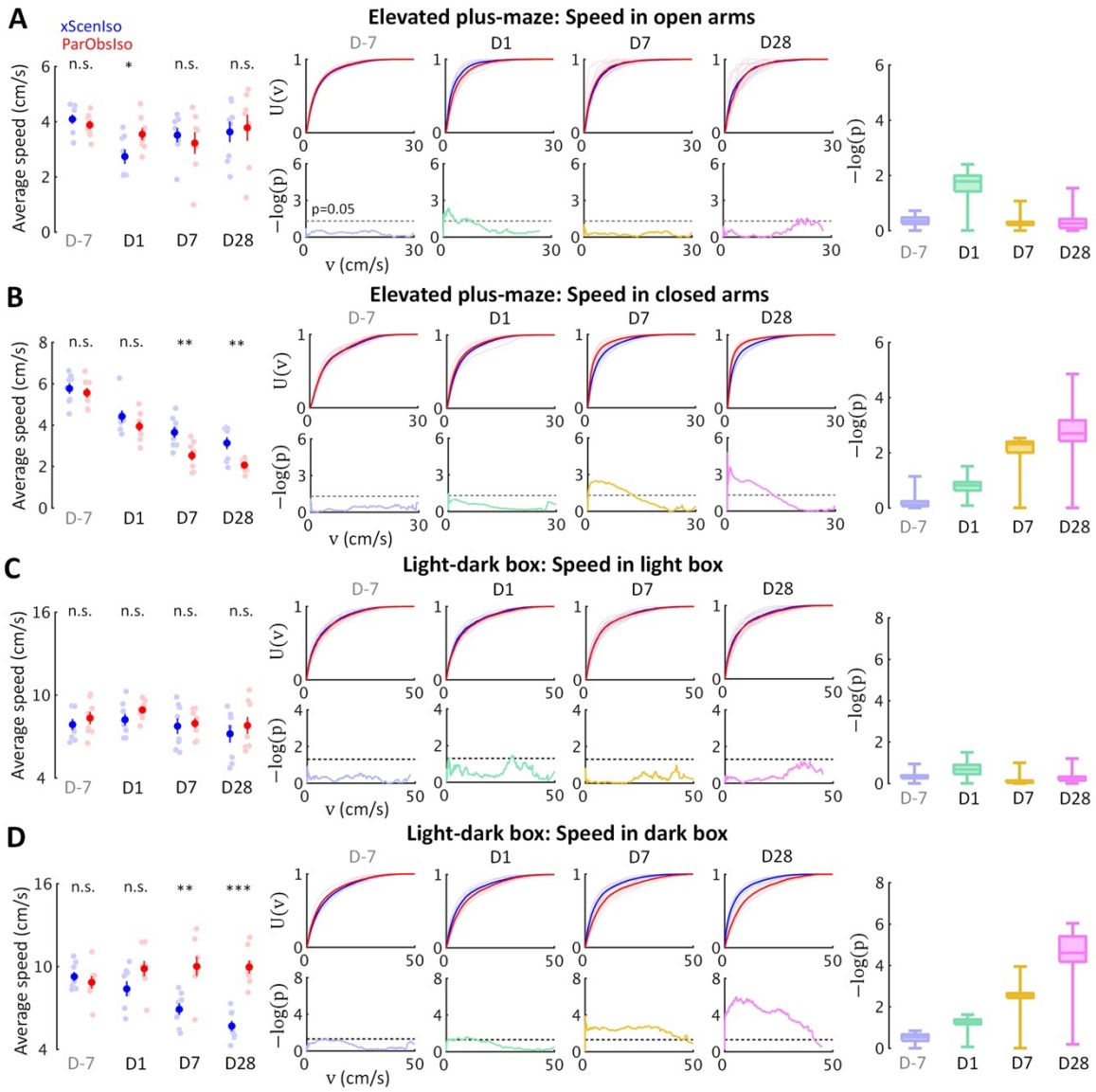

Figure 6. Gradually increasing anxiety and acute fear reaction were untangled in standard behavioral tests as different psychological components with distinctive developments. Locomotion speed shows acute difference only in stressor zones [open arms **(A)** and light area **(C)**], but incubated differences in stressor-free zones [dark area **(B)** and closed arms **(D)**].

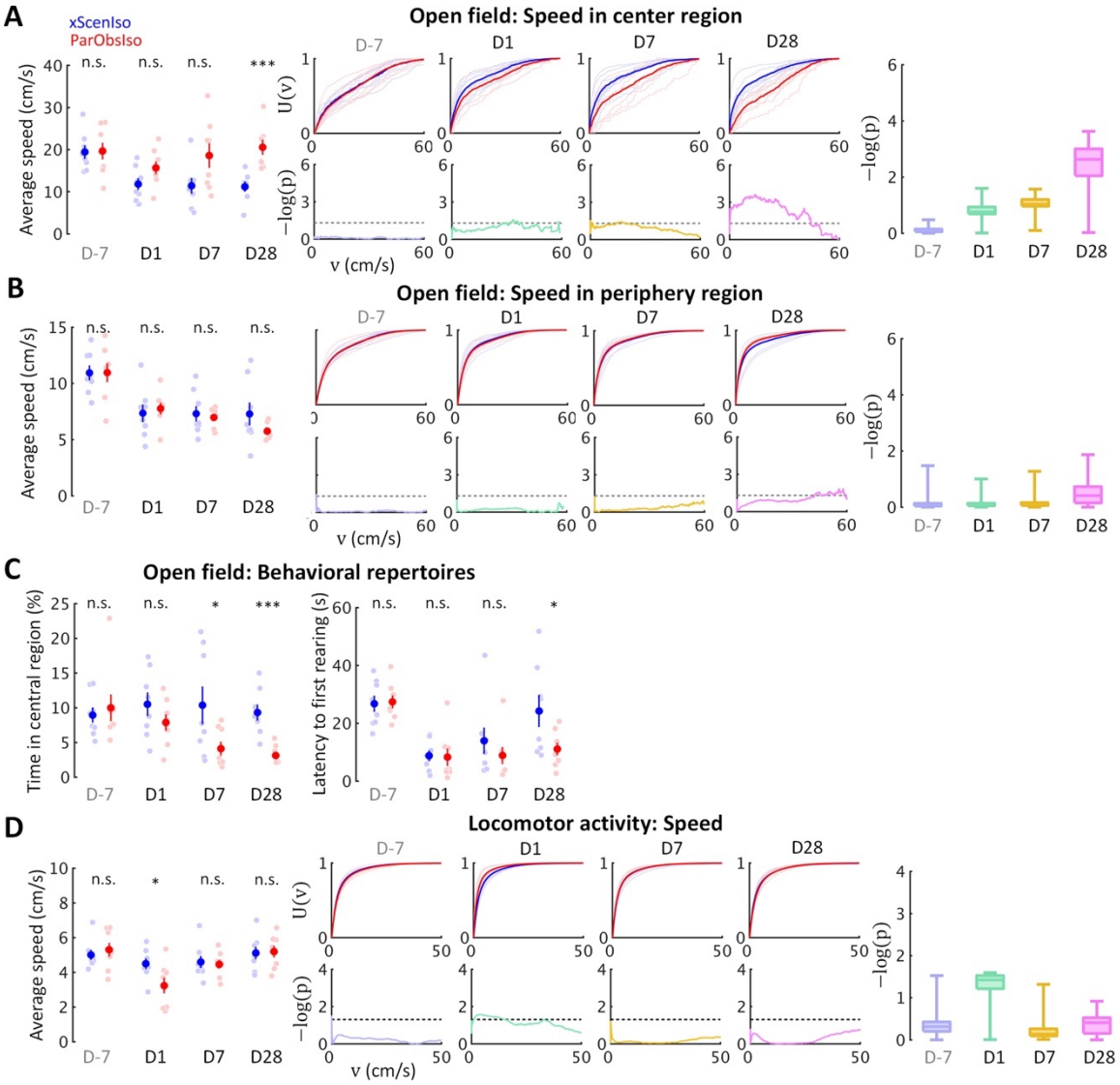

Figure 7. Behavioral testing in the open field test and locomotor activity test confirms distinctive psychological substrates and their corresponding development patterns. (A) Anxiety is evident in the open field test through a delayed onset of locomotor speed differences in the center region with higher spatial uncertainty. **(B)** The differences of locomotor speed observed in the center region did not occur in the periphery region with lower spatial uncertainty. **(C)** Less time spent in the central region by ParObsIso mice suggests their avoidance of a region with high special uncertainty, while shorter latency to their first rearing indicates their higher exploratory motivation. **(D)** In the locomotor activity test without stressors, acute effects of activity reduction recovered in the later post-traumatic period.

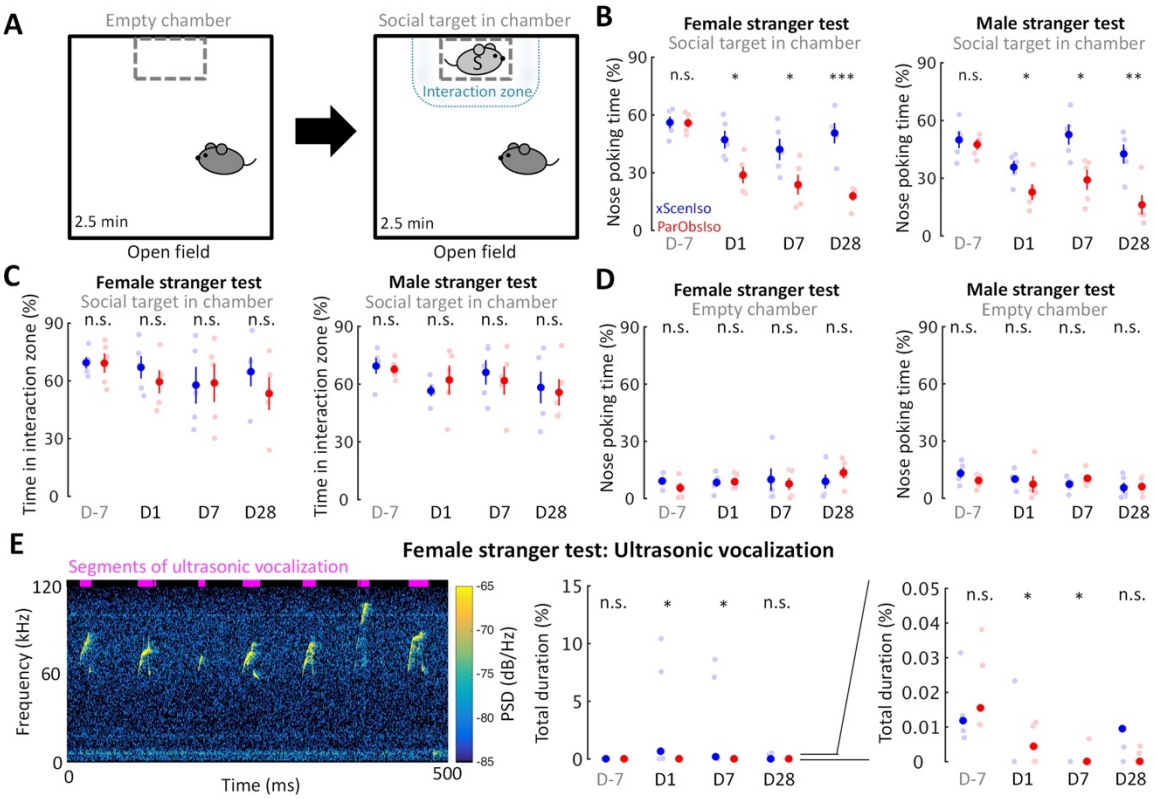

Figure 8. Acute psychosocial trauma decreases social interest. (A) The active social interaction test with consecutive non-social and social phases. During the social phase, motivation for social contact toward a stranger mouse (light gray S) was evaluated as the time spent for social approaches of nose poking and the time spent in the delineated interaction zone. **(B)** ParObsIso mice made fewer nose poking to both female (left) and male (right) strangers. **(C)** There was no significant difference in the time spent in the interaction zone during the social phase, suggesting a decrease of social interest instead of an active social avoidance. **(D)** There was no significant difference in the time spent of nose poking during the non-social phase, confirming that the observed differences of nose poking time stemmed from a specifically social root. **(E)** Spectrogram of short but conspicuous ultrasonic vocalizations emphasizes a specific behavioral repertoire during the social session in the female stranger test of a xScenIso mouse on Day1. More vocalization was recorded from xScenIso mice than ParObsIso mice on Days 1 and 7. Reduced ultrasonic vocalization during the social session of the female stranger test in ParObsIso mice attests to diminished social communication. Note that data points greater than 0.05% are not visible in the right panel which zoom in the data of the middle panel to emphasize the data distributions in the range of 0–0.05%. Data points and median, one-tailed Mann-Whitney U test; PSD, power spectral density.

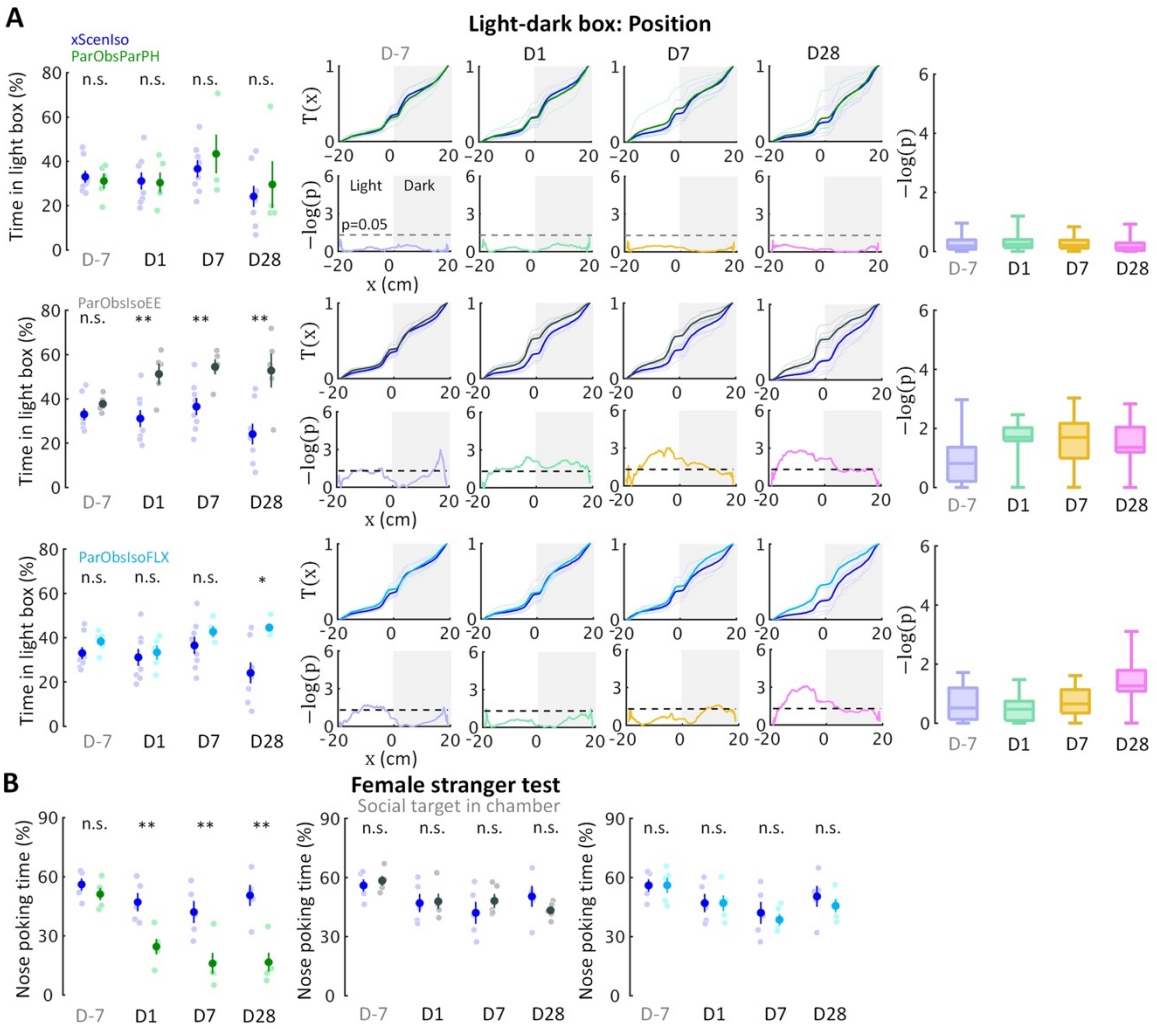

Figure 9. Developments of emotional and social differences are not inter-dependent. (A) Positions in the light-dark box test indicate that ParObsParPH mice did not develop the chronic stress reactions, ParObsIsoEE mice developed chronic stress reactions which were stronger than that of ParObsIso mice in the early phase, and ParObsIsoFLX developed stress reactions in the late phase. **(B)** Nose poking times in the female stranger test indicate that ParObsParPH, but not ParObsIsoEE and ParObsIsoFLX, mice develop the social differences of ParObsIso mice.

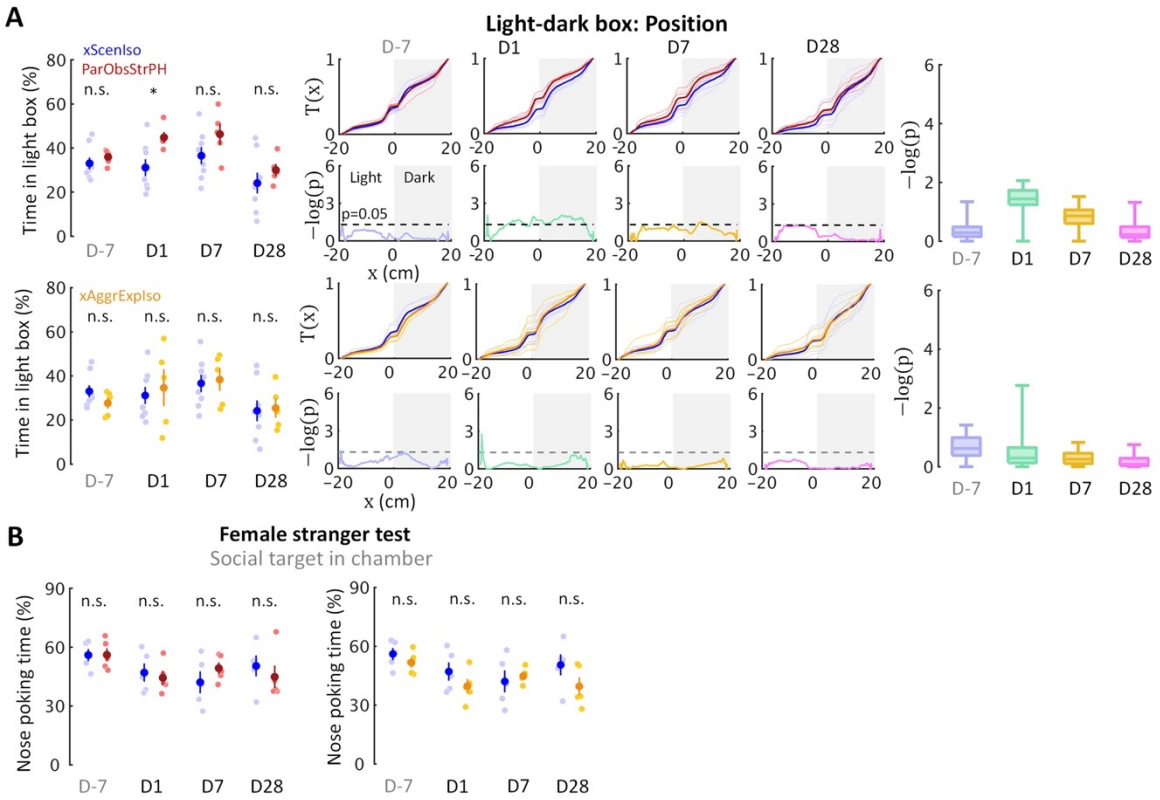

1509

1510 **Figure 10. Control experiments identify necessity of relationship-dependent vicarious**
1511 **defeat for anxiety incubation. (A)** Positions in the light-dark box test indicate that both
1512 xAggrExpIso and ParObsStrPH mice did not develop the behavioral differences in the late
1513 phase, although ParObsStrPH mice displayed the difference in the early phase. **(B)** Nose
1514 poking times in the female stranger test indicate that xAggrExpIso and ParObsStrPH mice did
1515 not develop the social differences.

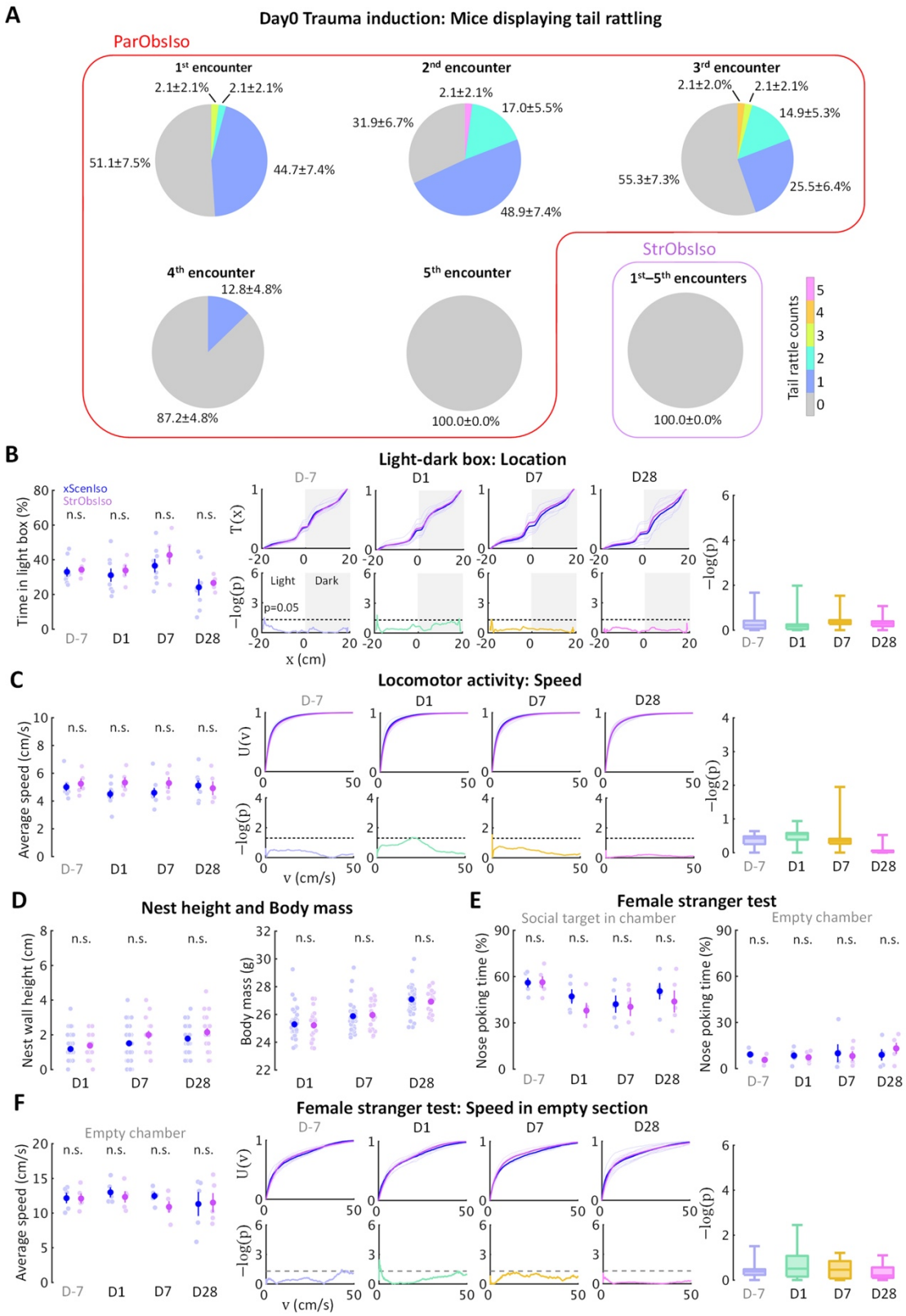

Figure 11. Social relationship in trauma induction determines stress development. (A) Social relationship increased emotional impact, evidenced by tail rattling behavior during trauma induction. **(B–F)** No significant acute or chronic difference was found in StrObsIso mice.

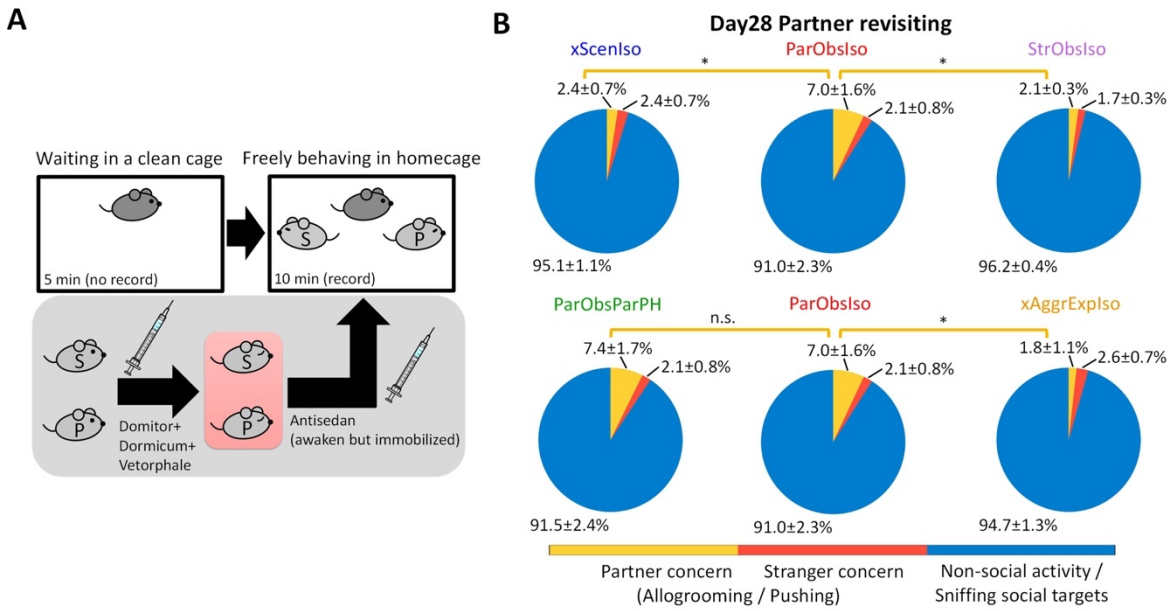

Figure 12. Long-term memory of partnership correlates with anxiety incubation. (A) The partner-revisiting test. A stranger mouse (light gray S) and the previously pair-housed partner (light gray P), both immobilized, were presented as social targets. Pink rectangle, heating pad. **(B)** ParObsIso and ParObsParPH mice showed significantly longer allogrooming or pushing their partners (yellow, % of time spent in partner concern behavior) than either xScenIso, xAggrExpIso, or StrObsIso mice. Standard errors were calculated from bootstrapped data.

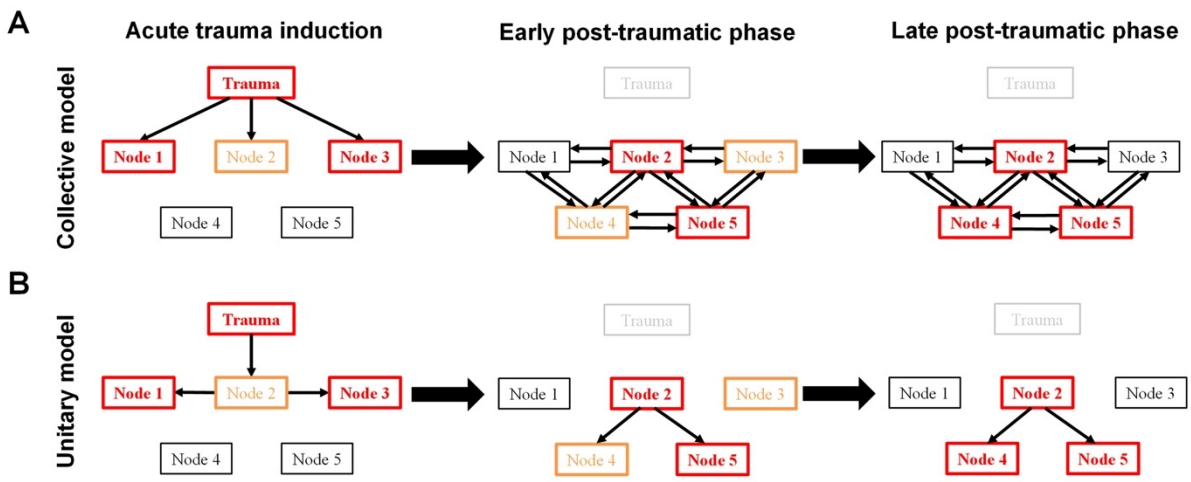

Figure 13. **Two conceptual models of the post-traumatic stress incubation process. (A)** In the collective model, different psychological elements (Node #, a type of emotion or cognition) influence each other during different phases of stress incubation. **(B)** In the unitary model a single common factor underlies the development of post-traumatic behaviors. Orange and red boxes represent medium and strong trauma-induced differences, respectively. It is assumed that each psychological element can be connected to an associated neural substrate with trauma-induced dynamic changes.

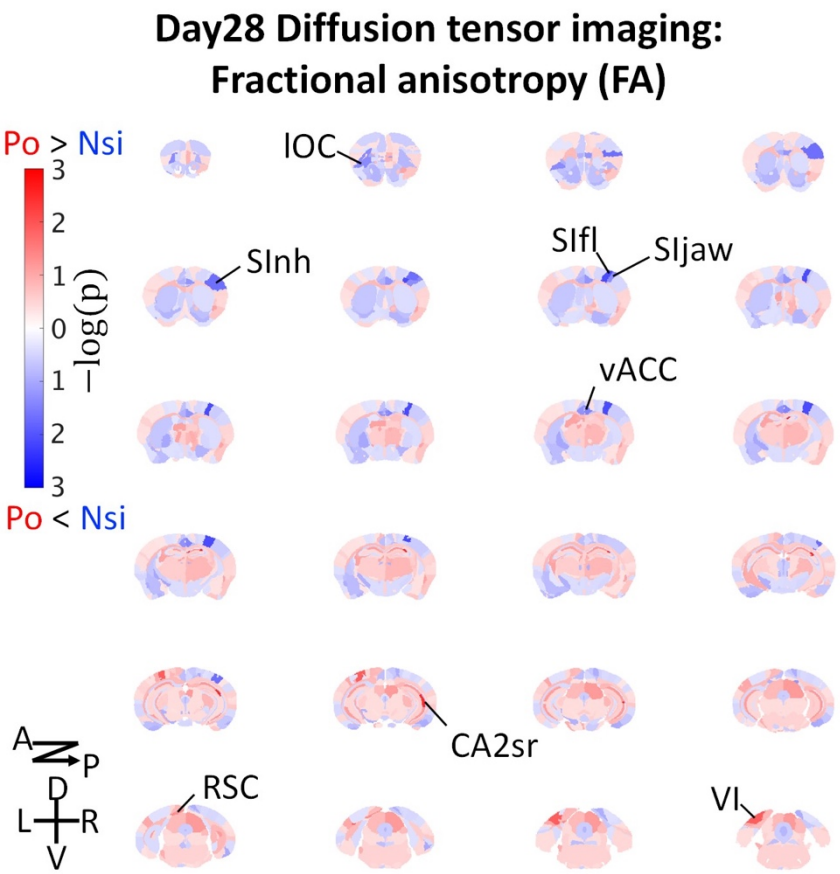

Supplemental Figure 1. Brain-wide microstructural changes measured by DTI fractional anisotropy. Po, ParObsIso mice; Nsi, xScenIso mice; -log(p), statistical significance through a two-population Student's t-test; A, anterior; P, posterior; D, dorsal; V, ventral; L, left; R, right; lOC, lateral orbital cortex; SInh, non-homunculus region of the primary sensory cortex; SIfl, forelimb region of the primary sensory cortex; SIjaw, jaw region of the primary sensory cortex; vACC, ventral region of the anterior cingulate cortex; CA2sr, stratum radiatum of the hippocampal cornu ammonis (CA) 2 area; RSC, the retrosplenial cortex; VI, the primary visual cortex.

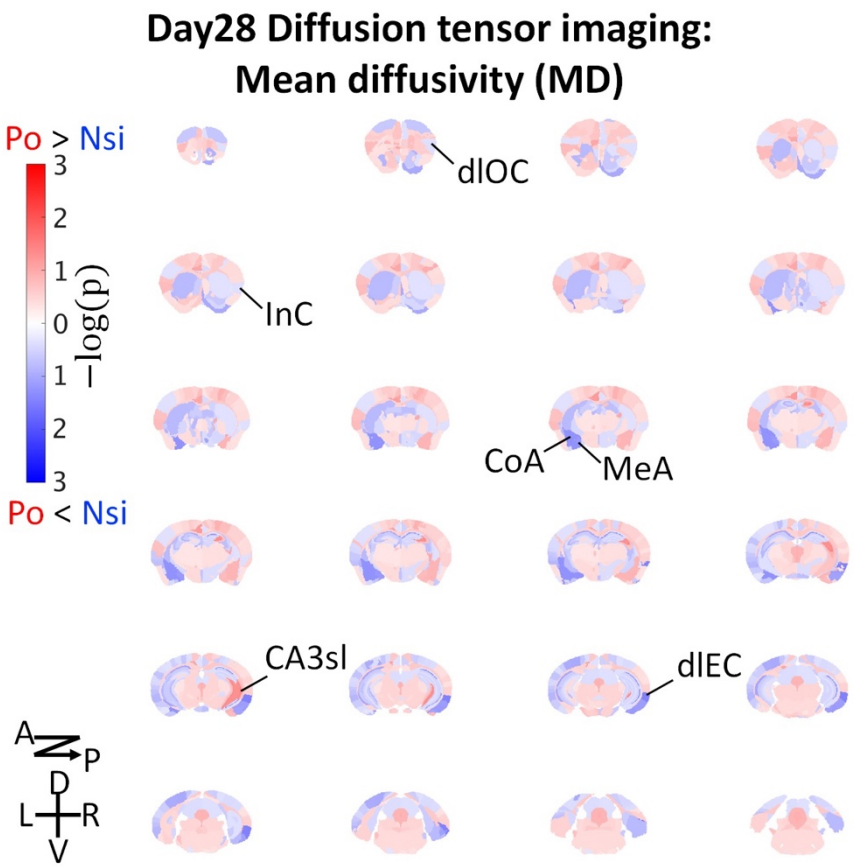

Supplemental Figure 2. Brain-wide microstructural changes measured by DTI mean diffusivity. dlOC, dorsolateral orbital cortex; InC, the insular cortex; CoA, the cortical amygdalar nucleus; MeA, medial amygdalar nucleus; CA3sl, stratum lucidum of the hippocampal CA3 area; dlEC, dorsolateral entorhinal cortex.

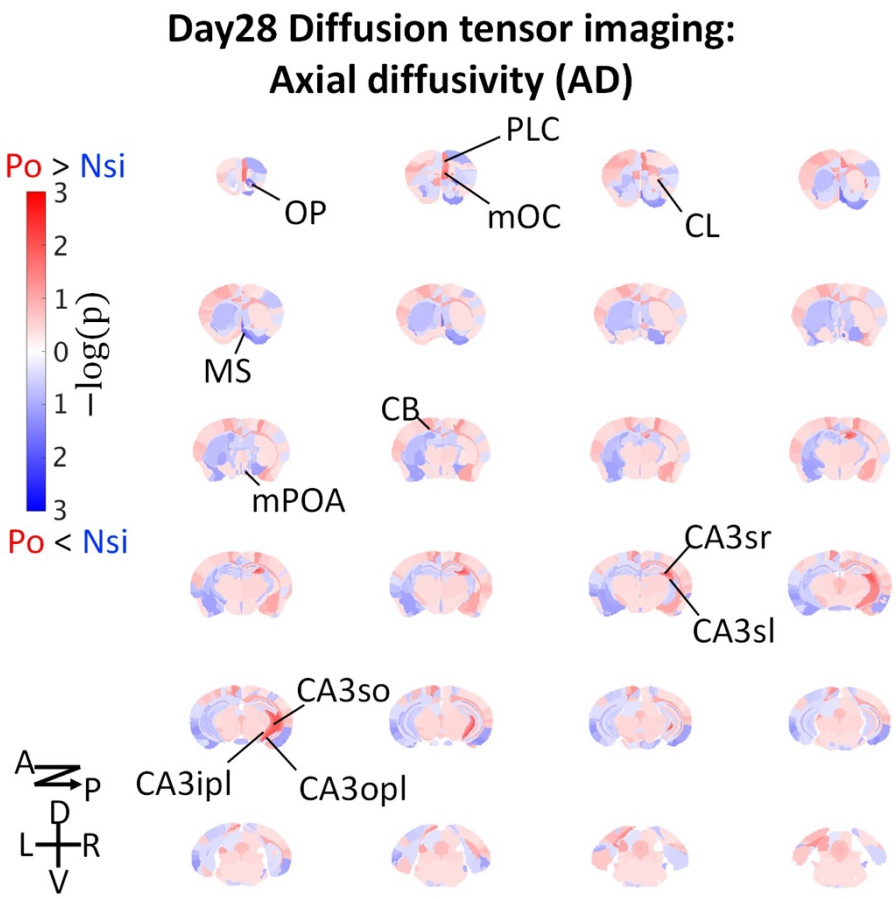

Supplemental Figure 3. Brain-wide microstructural changes measured by DTI axial diffusivity. OP, olfactory peduncle; PLC, prelimbic cortex; mOC, medial orbital cortex; CL, claustrum; MS, medial septal complex; mPOA, medial preoptic area; CB, cingulum bundle; CA3sr, stratum radiatum of the hippocampal CA3 area; CA3sl, stratum lucidum of the hippocampal CA3 area;CA3so, stratum oriens of the hippocampal CA3 area; CA3ipl, inner pyramidal layer of the hippocampal CA3 area; CA3opl, outer pyramidal layer of the hippocampal CA3 area.

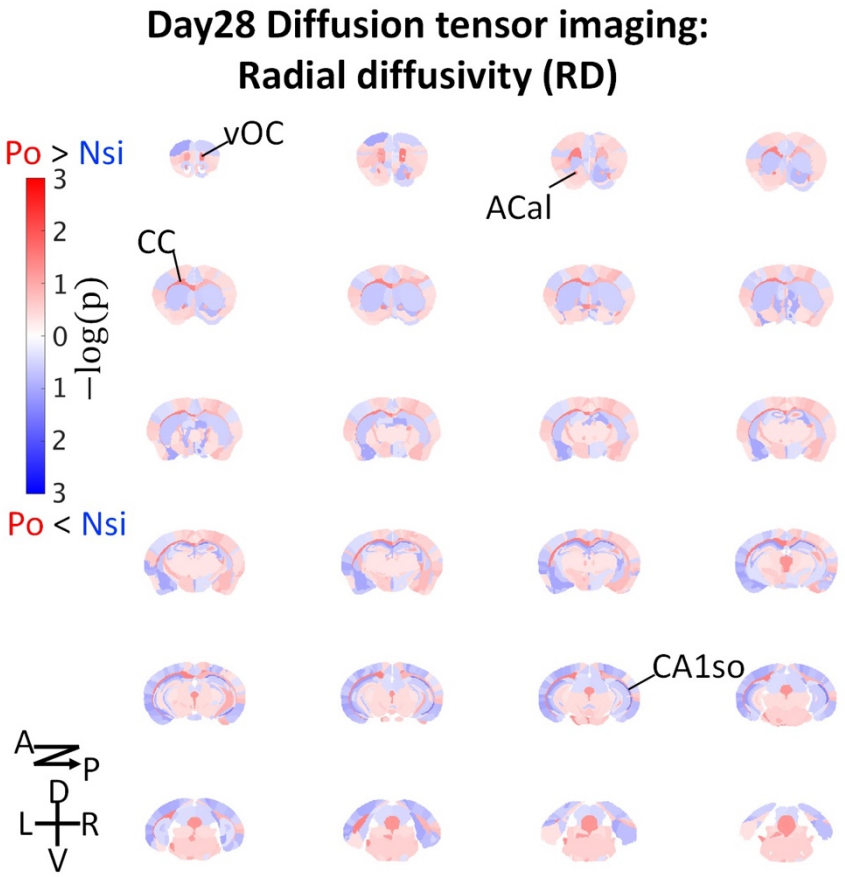

1559

1560 **Supplemental Figure 4. Brain-wide microstructural changes measured by DTI radial**
1561 **diffusivity.** vOC, ventral orbital cortex; ACal, anterior limb of the anterior commissure; CC,
1562 corpus callosum; CA1so, stratum oriens of the hippocampal CA1 area.

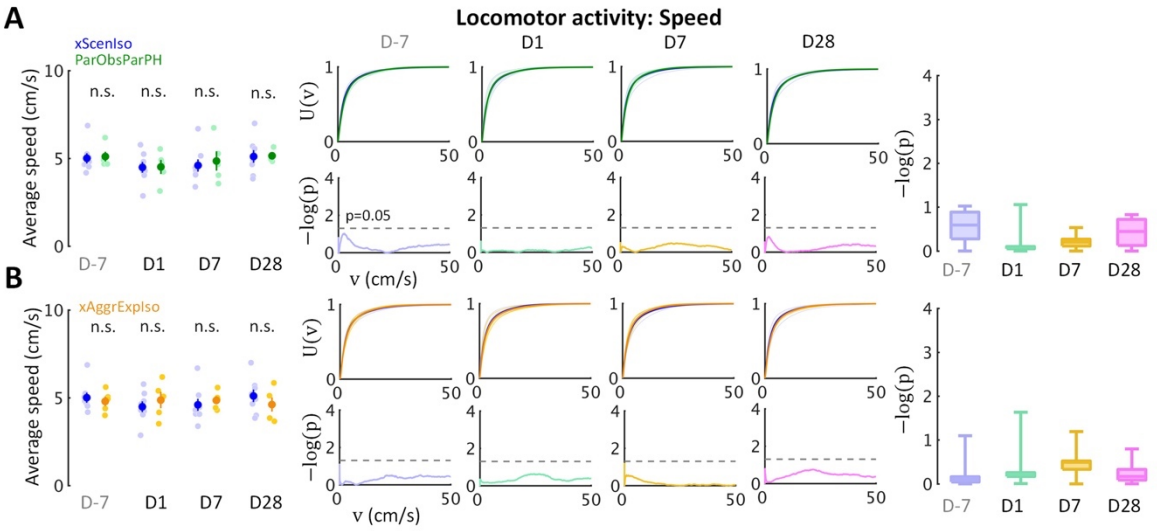

Supplemental Figure 5. Locomotor activity tests in control experiments agree with the conclusions of spontaneous behaviors given from the light-dark box tests. (A) The results of ParObsIsoFLX mice. **(B)** The results of ParObsStrPH mice.

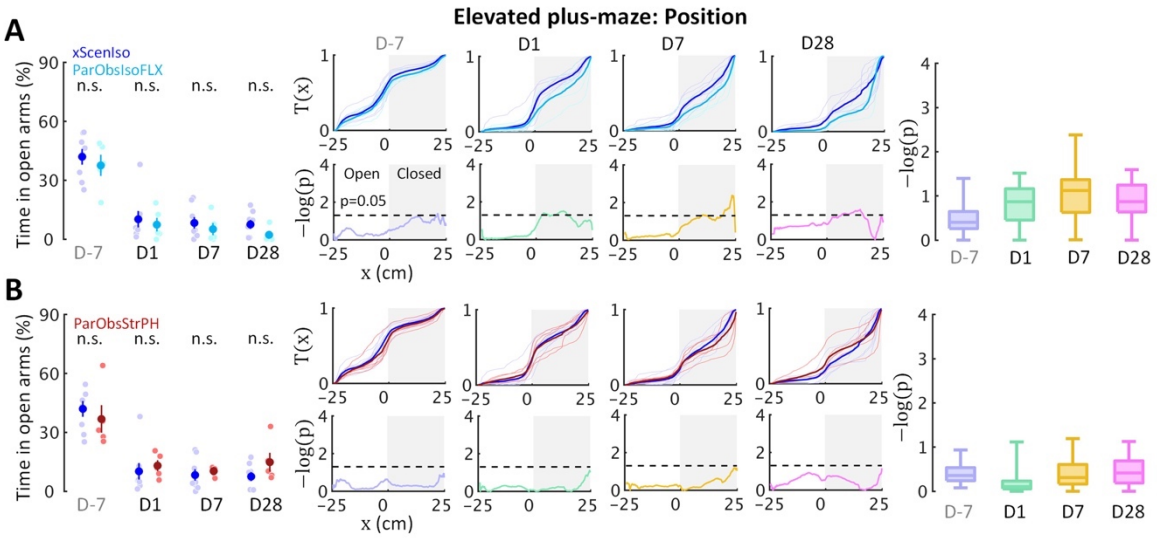

Supplemental Figure 6. Elevated plus-maze tests in control experiments agree with the conclusions of spontaneous behaviors given from the light-dark box tests. (A) The results of ParObsParPH mice. **(B)** The results of xAggrExpIso mice.

1571 **Supplemental Video 1.** Landscape in the 4-D state space of local likelihood of caffeine-
1572 injected behaviors in the light-dark box test.

1573 **Supplemental Video 2.** Landscape in the 4-D state space of local likelihood of foot-shocked
1574 behaviors in the light-dark box test.

1575 **Supplemental Video 3.** Landscape in the 4-D state space of local likelihood of control
1576 behaviors in the light-dark box test.

1577 **Supplemental Video 4.** Landscape in the 4-D state space of local likelihood of caffeine-
1578 injected behaviors in the elevated plus-maze test.

1579 **Supplemental Video 5.** Landscape in the 4-D state space of local likelihood of foot-shocked
1580 behaviors in the elevated plus-maze test.

1581 **Supplemental Video 6.** Landscape in the 4-D state space of local likelihood of control
1582 behaviors in the elevated plus-maze test.

1583 **Supplemental Video 7.** Social apathy is an observed behavioral characteristic of ParObsIso
1584 mice. Examples of 30-s recordings during the social session in the female stranger test on
1585 Day1. First scene, xScenIso mouse; Second scene, ParObsIso mouse.

1586 **Supplemental Video 8.** Illustration of behavioral characteristics that were specific to observer
1587 mice during trauma induction when their partners were attacked. First scene, tail rattling during
1588 aggressive encounter; Second scene, tail rattling during aggressive encounter (4x slower);
1589 Third scene, hiding under bedding material with the partner during resting. These behaviors
1590 were not observed if a stranger mouse got attacked.

1591 **Supplemental Video 9.** Illustration of rebound reaction of a ParObsIso mouse to its previously
1592 pair-housed partner during the partner-revisiting test.